



**The University of Queensland**

**Stress Analysis of a New Lightweight Piston for X2**

By  
David E. Gildfind

Departmental Report Number 2009/16

Division of Mechanical Engineering,  
School of Engineering,  
The University of Queensland,  
Australia.

4<sup>th</sup> of December, 2008

## Summary

A new lightweight piston has been designed for X2. The piston will be used to develop a tuned free piston driver condition which should increase the useful supply time of driver gas. The new piston retains the interfacing geometry of the existing 35kg piston, but has had significant amounts of mass removed where practical.

The piston strength was assessed for two load cases: an 80MPa ultimate pressure load applied to the front face of the piston to represent driver gas loading, and a 20MPa reservoir pressure loading applied inside the piston to represent pressure loading for the piston on the launcher. The piston was analysed using a symmetric solid finite element model.

The 80 MPa driver pressure load case was shown to be critical. The Von Mises stress was determined to be generally less than the allowable yield stress of the piston. Some locations on the solid model had stresses slightly exceeding the yield stress. The model was therefore reanalyzed using a non-linear material model, where it was shown that peak stresses fell below the ultimate allowable stress in all places.

The piston was shown to be able to resist the 20MPa reservoir pressure loading with minimal deformation (<0.05mm) at the seals, thus avoiding pre-launch due to leakage.

The piston was not assessed for impact or dynamic pressure loading. The design relies on avoiding piston impact into the end of the tube at high velocities. If this occurs, the tube will contain the piston, but the piston is likely to be irreparably damaged. The 2x safety factor applied in static analyses is expected to provide coverage against higher stresses that may occur under the actual dynamic pressure loading conditions. Further, the piston material is expected to have higher strength at high strain rates, which will provide further protection against failure.

Initial testing to approximately 68% of limit load (27MPa peak driver pressure) demonstrated no structural damage to the piston. Further testing will increase applied loading to 100% of limit load (40MPa peak driver pressure), whereupon the piston will be re-examined.

It is recommended that future work should involve detailed analysis of the piston response to dynamic pressure and impact loading using an explicit finite element code. Coupled with accurate material properties for high strain rate loading, this will provide a better understanding of the response of the piston to the applied loads, permitting a more optimised design in future.

## Table of Contents

1	Introduction	1
2	Overview of existing 35kg X2 piston	2
3	Overview of lightweight X2 piston	4
4	Materials	5
4.1	Piston	5
4.2	Load ring	6
4.3	Brass holder	6
4.4	Wear rings and chevron seal	7
4.5	Steel tunnel parts	7
5	Load cases.	8
6	Finite element analysis	9
6.1	Analysis software	9
6.2	Failure criteria	9
6.3	Symmetric finite element solid model – static analysis	9
6.3.1	Introduction	9
6.3.2	Finite element mesh	10
6.3.3	Interfaces	12
6.3.4	Loads and boundary conditions	12
6.3.5	Results	16
7	Analytical Stress Analysis	23
7.1	Overview	23
7.2	Buckling analysis	23
7.3	Reservoir Hoop Stress Finite Element Model Validation	24
7.4	Piston Impact	25
7.5	Dynamic Pressure Loading	26
7.6	Fatigue	26
8	Operational Experience	27
9	Recommendations	27
10	Conclusion	30
11	References	31
	Appendix A: Lightweight piston drawing set	32
	Appendix B: 7075-T6 Rod Mechanical and Physical Properties	42
	Appendix C: DOTMAR Nylon 6 Oil Filled Cast Properties	43
	Appendix D: MATWEB Nylon 6 Oil Filled Cast Properties	44
	Appendix E: X2 Lightweight Piston Initial Blanked Off Shot Details (Extract From Unpublished Test Report)	46

# **1 Introduction**

This report presents a structural analysis of a new lightweight piston for the X2 expansion tube. Previous flow condition analyses have shown that high total pressure flow conditions require a much longer duration of driver supply pressure than that which is currently achieved with the existing X2 35kg piston. A piston dynamics study indicated that a lightweight piston was required, in the order of 10kg total mass. Design constraints on the new piston primarily stemmed from the requirement that the piston be compatible with the existing launcher arrangement, therefore the interfacing geometry of the piston was required to be mostly identical. Mass was removed from suitable areas, and the new piston was assessed for strength. The results of the stress analysis of the piston are contained herein.

## 2 Overview of existing 35kg X2 piston

The existing piston arrangement is shown in Figure 1, Figure 2, and Figure 3 (CAD models taken from [1]). The axis system is shown in Figure 1 and Figure 2; y corresponds to the forward (driver gas exposed) face of the piston. Referring to Figure 3, it can be seen that there is a large mass of aluminium that may potentially be removed whilst preserving interfacing geometries.

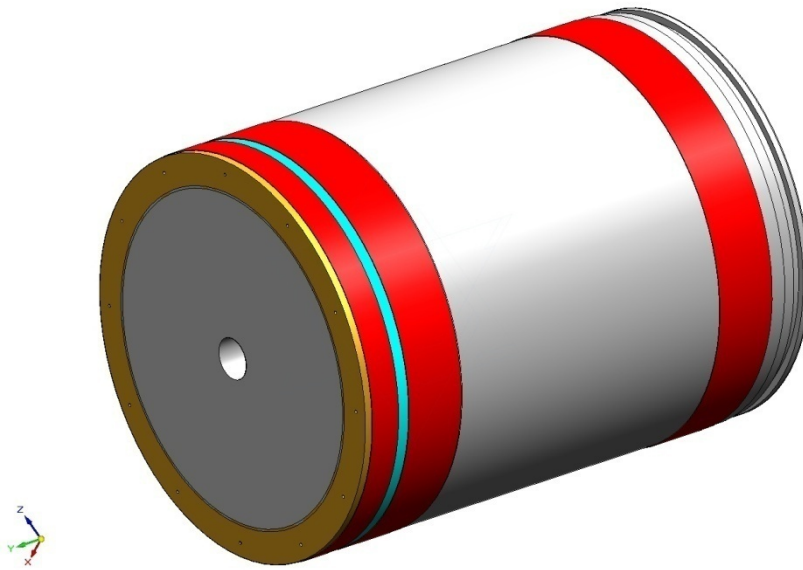


Figure 1: Piston assembly section view (brass seal holder - brass; seals – red; load ring – blue).

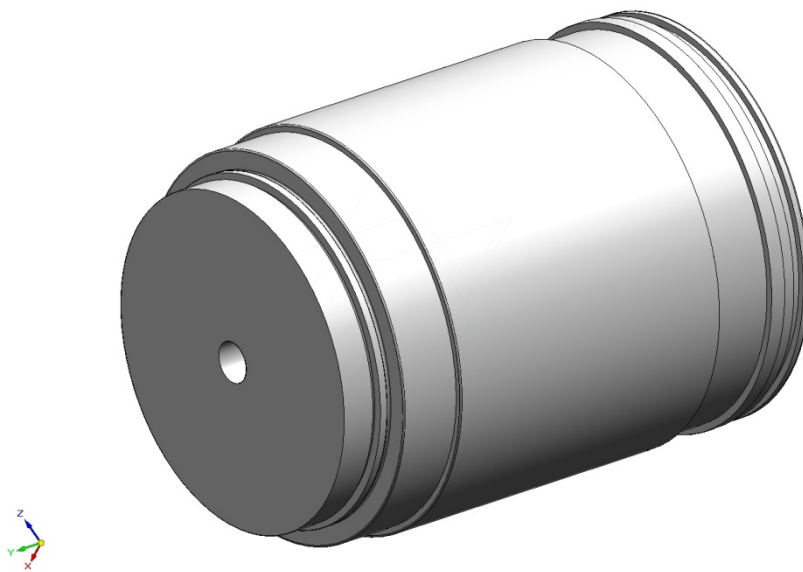


Figure 2: Piston body.

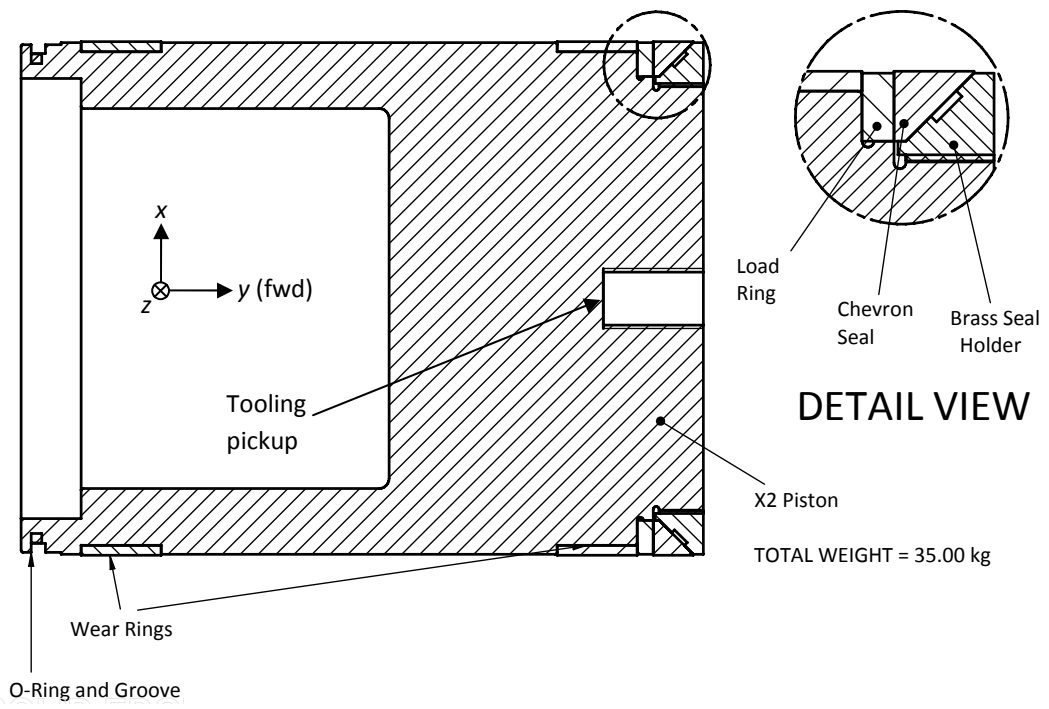


Figure 3: Piston assembly section view.

### 3 Overview of lightweight X2 piston

Detailed drawings for the new lightweight piston are attached in Appendix A. An assembly view of the lightweight piston, and a view of the piston body, are shown in Figure 4 below. The entire piston assembly nominally weighs 10.683kg. Referring to Figure 3 above, the weight reduction was achieved by making the following changes:

1. Reducing the depth of the piston head.
2. Reducing the hole depth of the tooling pickup.
3. Reducing the width of the wear rings (from 40mm to 30mm).
4. Removing material from the piston outer surface between the two wear rings.
5. Cutting out material from underneath the wear bands.

It is noted that the forward inner radius of the piston had to be increased to reduce peak stresses. This increased radius required incorporation of a chamfer on the piston launcher to ensure clearance. The material removal will have a negligible impact on launcher strength and is considered acceptable by inspection.

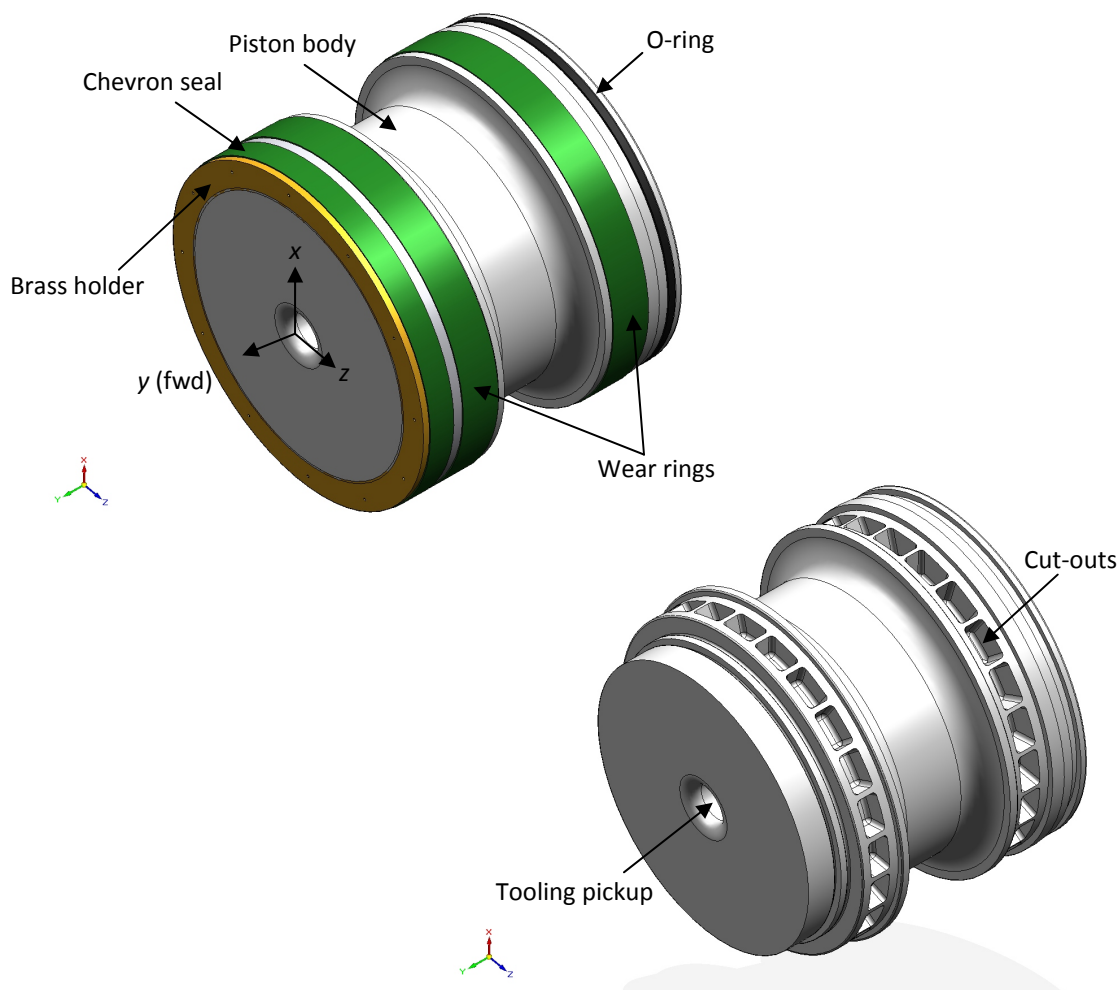


Figure 4: Lightweight piston views.

## 4 Materials

### 4.1 Piston

The piston is manufactured from 7075-T6 aluminium alloy, for its high strength-to-weight, and for its reasonable material cost. The diameter of the new piston will be the same as the old piston (256.8mm), and the basic piston form will be achieved by machining it on a lathe. For this application, a suitable raw material form is aluminium rod, which can be supplied up to, and in excess of, the required piston diameter. The raw rod material is originally manufactured to large lengths (i.e. several meters), so a piece at the required length for this piston (< 300mm) is obtained by ordering a section of appropriate length be cut by the supplier.

Detailed mechanical and physical properties for the specific aluminium rod material were not available, nor was a guaranteed material specification. For the purposes of this design, properties were taken from MIL-HDBK-5H [2], Table 3.7.4.0(d) (refer Appendix A). This reference provides mechanical and physical properties for rod diameters between  $0 < D \leq 4$ ". For the range of diameters shown, it can be seen that quoted properties either remain unchanged (in grain direction L), or deteriorate slightly (in transverse direction L-T), with increasing rod diameter. Therefore, the largest quoted rod diameter will be used (4"), and it will be assumed that these properties are also applicable to the rod material size required for this piston (approximately 10" diameter).

The more conservative A-basis allowables will be used (these allowables are derived from a broader band of test results). MIL-HDBK-5H provides properties in both L and L-T orientations (i.e. relative to grain direction, where applicable); since the material will be analysed numerically assuming isotropic mechanical properties, the minimum of each of these values will be assumed to apply in all directions. Finally, it will be assumed that quoted allowables are true stresses, which is reasonable given the relatively small elongation at failure. In addition to the above three conservative assumptions, any potential discrepancies between assumed and actual material mechanical properties are considered to be acceptable in light of the large (2x) safety factor applied to loads used for certification of the design.

Table 1 below presents the assumed mechanical and physical properties for the 7075-T6 rod which will be used for this piston design. Original empirical units from MIL-HDBK-5H are quoted, as well as the same quantities in metric units. Tangent modulus is calculated assuming constant modulus between material yield and failure, which is reasonable for this type of aluminium alloy which tends to plastically deform at a constant rate until failure.



Property	Description	Value		Notes
		Empirical	Metric	
$F_{tu}$	Ultimate tensile strength	69 ksi	476 MPa	A-basis, L-T value, 3.001-4.000" DIA.
$F_{ty}$	Yield tensile strength	60 ksi	414 MPa	A-basis, L-T value, 3.001-4.000" DIA.
$F_{cy}$	Yield compressive strength	64 ksi	441 MPa	A-basis, L value.
$F_{su}$	Ultimate shear strength	46 ksi	317 MPa	A-basis.
$e$	Strain at failure	0.07 (7%)	0.07 (7%)	A-basis.
$E$	Young's modulus	10,300 ksi	71.0 GPa	Smaller of $\bar{E}$ and $E_c$ .
$E_t$	Tangent modulus	140 ksi	965 MPa	$E_t = (F_{tu} - F_{ty}) / (e - F_{ty} / E)$ .
$G$	Shear modulus	3,900 ksi	26.9 GPa	
$\mu$	Poisson's ratio	0.33	0.33	
$\rho$	Density	0.101 lb/in <sup>3</sup>	2,796 kg/m <sup>3</sup>	

**Table 1: Mechanical and physical properties of 7075-T6 rod [2].**

## 4.2 Load ring

The load ring is manufactured from commercial aluminium (i.e., not a specific alloy of aluminium). It is not a highly stressed component, and its design is acceptable by inspection. The stiffness and mass properties of the load ring are assumed to be the same as those shown in Table 1, which is reasonable since density and stiffness do not vary significantly between different alloys of aluminium.

## 4.3 Brass holder

The brass holder is manufactured from cast aluminium bronze, specification C95810. Material properties for C95800 series copper alloy were used for the analysis, and were taken from [3]. Properties are shown in Table 2 below. It is noted that the strength of the brass holder is not assessed in this analysis; since the design remains unchanged from the existing 35kg X2 piston, it is passed by comparison. Therefore only material properties relevant to this analysis are presented (i.e. stiffness and density properties).

Property	Description	Value	Notes
$E$	Young's modulus	110 GPa	Tension direction.
$\mu$	Poisson's ratio	0.32	
$\rho$	Density	7,640 kg/m <sup>3</sup>	

**Table 2: Mechanical and physical properties of C95800 copper alloy [3].**

#### 4.4 Wear rings and chevron seal

The wear rings and chevron seal are all machined from Nylon 6 oil filled cast. Only the stiffness properties are required for these parts, since they are not strength critical. Properties are shown in Table 3 below.

Property	Description	Value	Notes
$E$	Young's modulus	2.28 GPa	Per Appendix B, compression direction, since these are bearing components.
$\mu$	Poisson's ratio	0.4	Per [4], Table H-1, for Nylon.
$\rho$	Density	1,135 kg/m <sup>3</sup>	Per Appendix B.

**Table 3: Mechanical and physical properties of Nylon 6 oil filled cast.**

#### 4.5 Steel tunnel parts

The steel tube walls are modeled in ANSYS as rigid boundaries. Steel is significantly stiffer than Aluminum, therefore this assumption is considered to be reasonable.

## 5 Load cases.

The piston was subject to two load cases:

1. LC1: Driver pressure loading. The maximum operational driver pressure for X2 is 40 MPa. This load was factored by 2x (to give 80 MPa) and applied to the front face of the piston. Basic piston sizing was performed from a static analysis of a 3D solid model.
2. LC2: Reservoir pressure loading. The maximum operational reservoir pressure loading for X2 is 10MPa, which acts on the walls of the piston when it is held in the launcher. This load was factored by 2x (to give 20 MPa) and applied to the inside walls of the piston. A static analysis of a piston solid model was performed to assess the piston strength and deformation under this applied loading.

The two load cases are summarized in Table 4:

Load case ID	Applied load	Safety factor	Factored load	Comments
LC1	$p_{\text{drv}} = 40.0 \text{ MPa}$	2.0	$p_{\text{drv},f} = 80.0 \text{ MPa}$	Maximum driver pressure. This load is considered for both static and dynamic cases. It is applied across the entire front face of piston.
LC2	$p_{\text{res}} = 10.0 \text{ MPa}$	2.0	$p_{\text{res},f} = 20.0 \text{ MPa}$	Maximum reservoir pressure, applied inside the piston cavity, between seal centrelines.

**Table 4: Factored piston loads.**

## **6 Finite element analysis**

### **6.1 Analysis software**

ANSYS Workbench 11.0 was used to perform the simulation.

### **6.2 Failure criteria**

The piston body was assumed to have yielded when the Von Mises stress, calculated by ANSYS, exceeded the material yield stress (414 MPa) from Table 1. The onset of material yield can be assessed using a linear structural analysis, however the final stress distribution is not accurate, since load will redistribute to the stiffer material which has not yielded.

Material yielding does not imply catastrophic failure. Failure was assessed by performing a static analysis using a nonlinear material model for the piston body. Failure was considered to have occurred when the Von Mises stress, calculated by ANSYS, exceeded the material ultimate tensile stress (476 MPa) from Table 1.

The piston body was designed to have zero yield for the two applied pressure load cases, LC1 and LC2, in Table 4. This would prevent any deformation of the piston at ultimate load, permitting repeated use of the piston (a deformed piston may require repair or scrapping).

It is the nature of finite element models (particularly solid models) that local stress peaks are observed due to the nature of the element formulation and the discrete nature of the mesh over the complex geometry. Where local stress concentrations indicated high stresses (exceeding yield) which appeared unrealistic, a secondary nonlinear analysis was used to confirm that the piston would not fail under this loading.

Considering the 2x safety factor applied to loads, the conservative material allowables selected in Table 1, and the non-yield criteria applied to the piston design, there is significant conservatism applied to the design.

### **6.3 Symmetric finite element solid model – static analysis**

#### **6.3.1 Introduction**

The lightweight piston is axisymmetric except for two features:

1. Outer surface cut-outs in the piston body (beneath the wear rings) spaced at 15 deg intervals around the axis of symmetry.
2. Venting holes in the brass holder, spaced at 30 deg intervals around the axis of symmetry.

For the purposes of the piston design, only the structural cut-outs in the piston body required consideration. The brass holder is an existing design which has already demonstrated satisfactory operational performance. It was incorporated in the finite element model of the piston assembly since it forms a significant part of the driver pressure load path. However, by inspection, local changes to its structural response due to the venting holes will not affect load transfer into the piston body.

Therefore a static analysis of a 1/24<sup>th</sup> slice of the piston was analysed. The chevron seal, load ring, and wear rings, were incorporated in the finite element model in order to more accurately simulate the boundary conditions on the piston body. For example, considering the reservoir pressure load case, if a rigid support is not applied at the wear strip locations, but instead directly to the piston body, then this will permit significant load transfer to the tunnel walls. However, in reality there are comparatively soft wear strips between the tunnel walls and the piston body. For the small deformations associated with the reservoir pressure loading, the expansion of the piston body will be accommodated by compression in the soft wear strips, therefore the actual load transfer to the tunnel will be negligible. These accessory items were incorporated with representative stiffnesses, however they were not assessed for strength.

It is noted that the brass holder is screwed onto the piston body. In the finite element model these two items were effectively bonded along the mid-thread surface. The brass holder was given appropriate material properties. This arrangement was selected so that the pressure load acting on the brass holder would be transferred into the piston body in a realistic manner. The actual thread was not assessed for strength, since an identical thread exists on the 35kg X2 piston, and is therefore acceptable by comparison.

### **6.3.2 Finite element mesh**

ANSYS was used to automatically generate a solid element mesh with element global edge length of 1.5mm. The mesh, which has 125,775 nodes and 54,462 elements, is shown in Figure 5 (with accessories) and Figure 6 (piston body only) below:

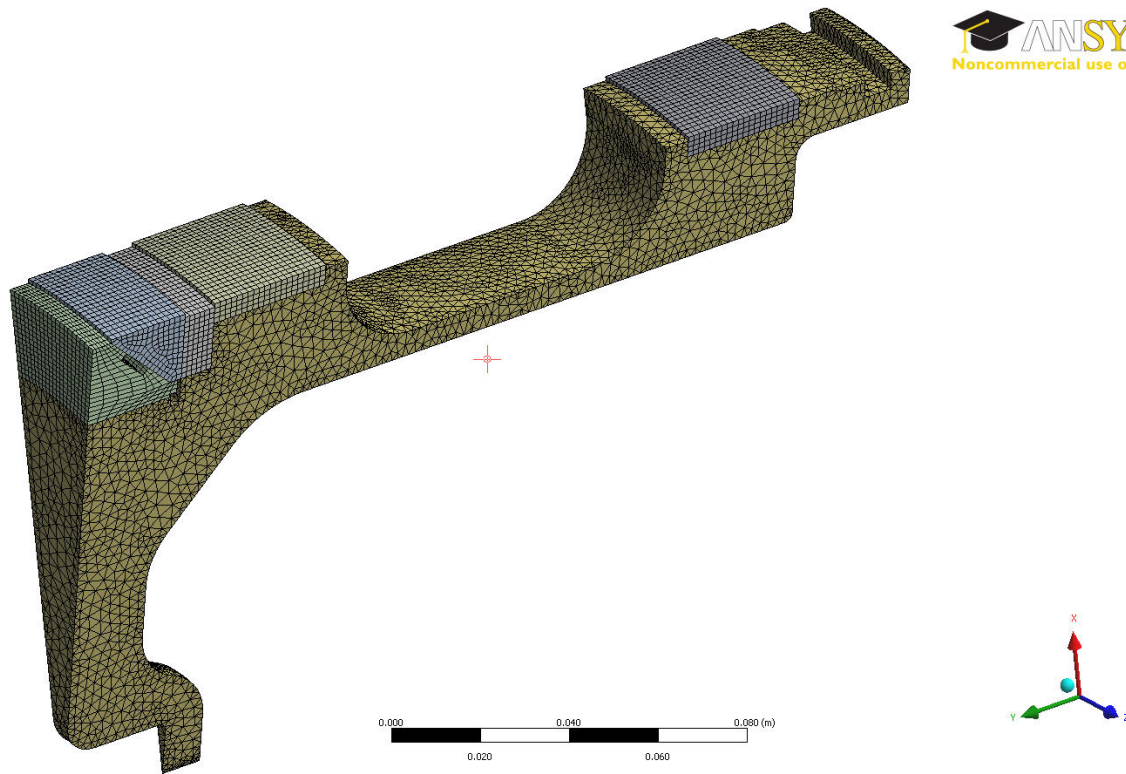


Figure 5: Solid mesh, 1/24<sup>th</sup> segment model, piston with accessories.

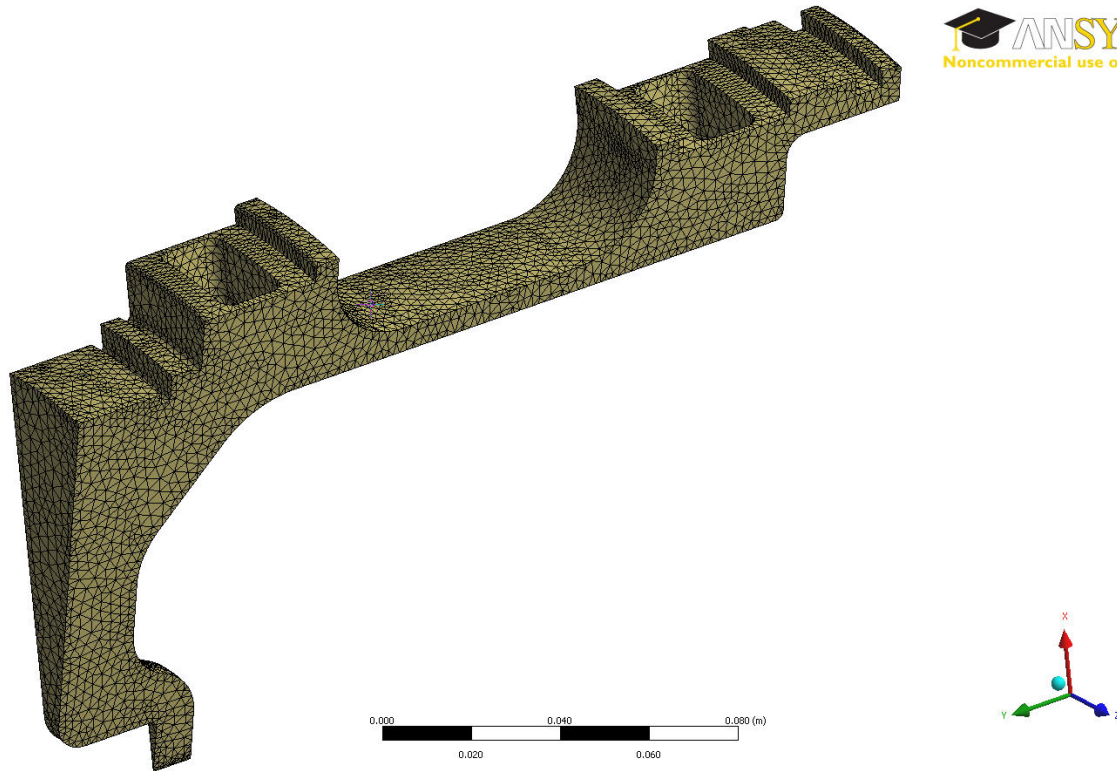


Figure 6: Solid mesh, 1/24<sup>th</sup> segment model, piston body only.

### 6.3.3 Interfaces

Different interface options are available in ANSYS, such as a bonded interface (surfaces stuck together), a frictionless interface (surfaces must remain on the same plane), a compression only interface (surfaces can separate but not pass through each other) etc. The type of interface determines whether the analysis is linear or not, since a contact-type interface must be solved iteratively. Two types of interface were selected in ANSYS:

1. Bonded interfaces: the interfaces between the piston body and the wear rings, the piston body to the load ring, and the piston body to the brass holder. This constrains the relative motion of the interfacing surfaces to behave like the surfaces are bonded.
2. No separation interfaces: all other interfaces, such as the chevron seal to the brass holder, the wear ring edges to the piston, the piston to the side of the load ring etc. This keeps the two surfaces coplanar, but allows in-plane movement.

### 6.3.4 Loads and boundary conditions

#### 6.3.4.1 80 MPa driver pressure loading

Referring to Figure 7 below, both radial cut planes are planes of symmetry. The piston geometry may slide in-plane, but not across either plane. Therefore, frictionless supports were applied along the two cut surfaces (coloured blue; one side is visible in Figure 7).

Piston geometry that lies along the axis of symmetry is only free to move along this axis, therefore a constraint was applied along this edge (a displacement constraint, coloured yellow).

The surfaces which interface with the tunnel – i.e. the two wear rings and the chevron seal – were also given frictionless constraints (coloured blue). This constraint is only approximate, since it can apply both tensile and compressive forces to these surfaces; the actual tunnel can only provide compressive resistance to these surfaces. The chevron seal and wear rings are very soft compared to the metallic components, therefore even if tensile stress arises within them, the small displacements involved will not result in the development of large forces. This simplification should therefore be acceptable, and is preferable since a compression-only support introduces additional non-linearity to the problem, which in this case would increase complexity unnecessarily.

An 80 MPa pressure loading (coloured red) was applied normal to all surfaces along the front face of the piston.

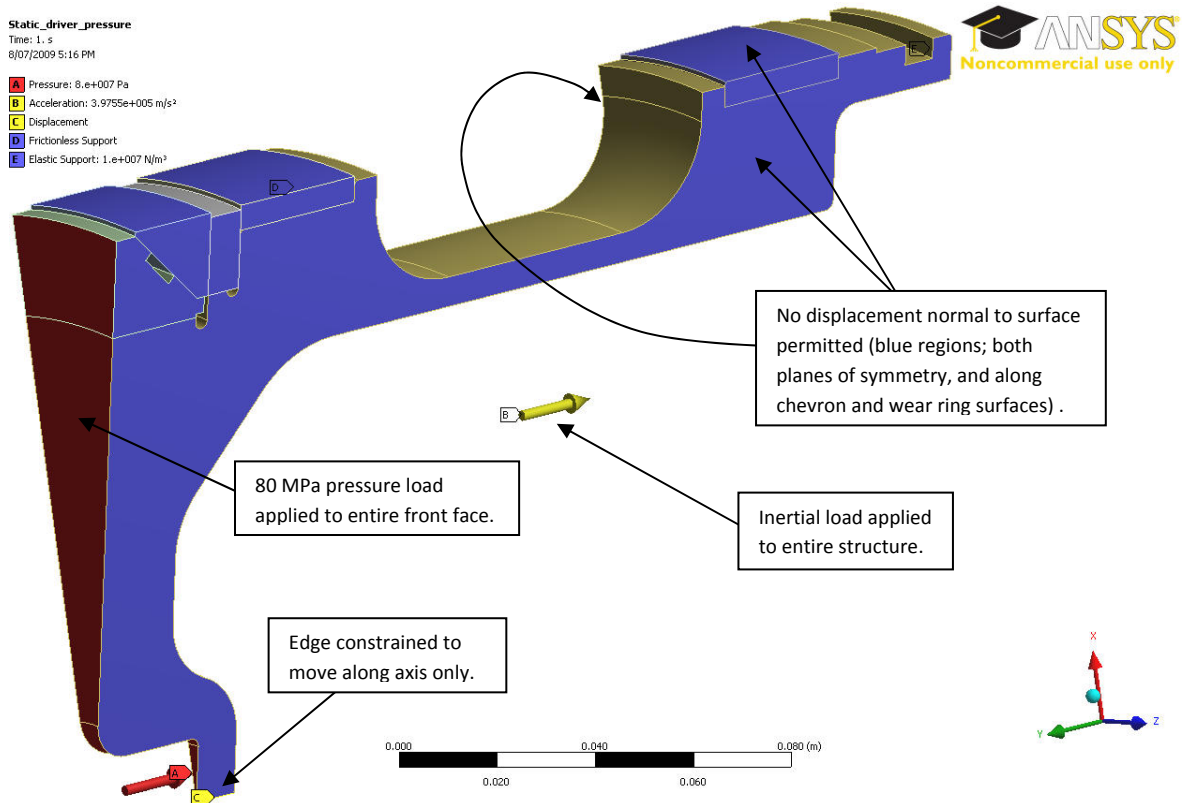


**Figure 7: Loads and boundary conditions, 80 MPa driver pressure load case.**

It is noted that this load case is actually, in reality, dynamic. The piston has velocity as it approached the end of the compression tube. The pressure builds up in front of the piston, slowing it down. However, for the detailed stress analysis of the piston body, a static analysis was performed. Resistance to the applied load was achieved by applying an inertial load to the structure. This load is applied as an acceleration, and is analogous to a gravity force. The inertia force models the stress state in the piston when it is subject to a steady acceleration due to the applied pressure force at one end, and ignores any transient variation in stress distribution due to stress waves moving through the piston structure.

The acceleration of the piston is calculated in Table 5 below. It is noted that the discrete nature of the finite element mesh is such that this acceleration cannot perfectly balance the applied pressure force, therefore an additional support is required in the direction of the applied load. An elastic support of stiffness  $1 \times 10^7 \text{ N/m}^3$  was applied to the rear face of the piston (not visible in Figure 7) to resist small residual forces, in order to avoid rigid body motion.



Notation	Description	Value	Units	Comments
P	Driver pressure	$80 \times 10^6$	Pa	Refer Table 4
D	Piston diameter	0.2558	m	Outer diameter of brass holder
A	Piston area	0.05139	m <sup>2</sup>	$A = \pi D^2 / 4$
F	Force on piston face	4,111,317	N	$F = PA$
m	Piston mass	10.478	Kg	Refer Appendix B
a	Piston acceleration	392,376	m/s <sup>2</sup>	$a = F/m$

**Table 5: Calculation of piston acceleration due to 80MPa driver pressure.**

Preliminary analysis indicated that there was indeed residual load resisted by this support, although it was small, indicating that the inertial force was correctly applied. However, a correction was applied to the acceleration body force to account for the discrepancy. The correction was calculated iteratively. Starting with the acceleration in Table 5, the following procedure was followed:

1. Calculate area of elastic support:  $A = \frac{\pi}{4} (251.8^2 - 234^2) \times \frac{1}{24} = 283.0 \times 10^{-6} \text{ mm}^2$
2. Run simulation. Determine displacement at elastic support.
3. Calculate corresponding support force:  

$$F = K\delta = (kA)\delta = 1 \times 10^7 \times 283.0 \times 10^{-6} \times \delta = 2,830 \times \delta$$
4. Calculate correction to acceleration:  

$$a = \frac{F}{m} = \frac{2,830 \times \delta}{(10.478 / 24)} = 6,482 \times \delta$$
5. Add to nominal acceleration:
6.  $a_{new} = a_{old} + a_{correction}$
7. Repeat steps 1 to 6 until residual support force is negligible.

The above procedure was adopted, with the corrected acceleration being 397,552 m/s<sup>2</sup>. Comparing this to Table 5, this constitutes a 1.3% error, which demonstrates that the acceleration load is correctly applied.

#### **6.3.4.2 20 MPa reservoir pressure loading**

Figure 8 below shows the loads and boundary conditions applied to the 1/24<sup>th</sup> axisymmetric piston model for the reservoir pressure load case. The same constraints were used as those described in Section 6.3.4.1, with the addition of a constraint against motion along the axis of symmetry in order to prevent rigid body motion. The reservoir pressure was applied normal to the inside surface of the piston along the entire constant radius section. Referring to the actual launcher design illustrated in Figure 9, the actual reservoir

pressure load only acts between the two o-ring seals, therefore the assumed loading area is conservatively large.

It is noted that once the piston is released from the launcher, the reservoir gas fills the entire cavity inside the piston, and acts across the entire inner surface. This load case was not assessed since it is similar to the driver pressure load case, but only 25% of the magnitude (and opposite direction). The piston strength with respect to reservoir pressure loading after launch is acceptable by comparison to the driver pressure load case, LC1.

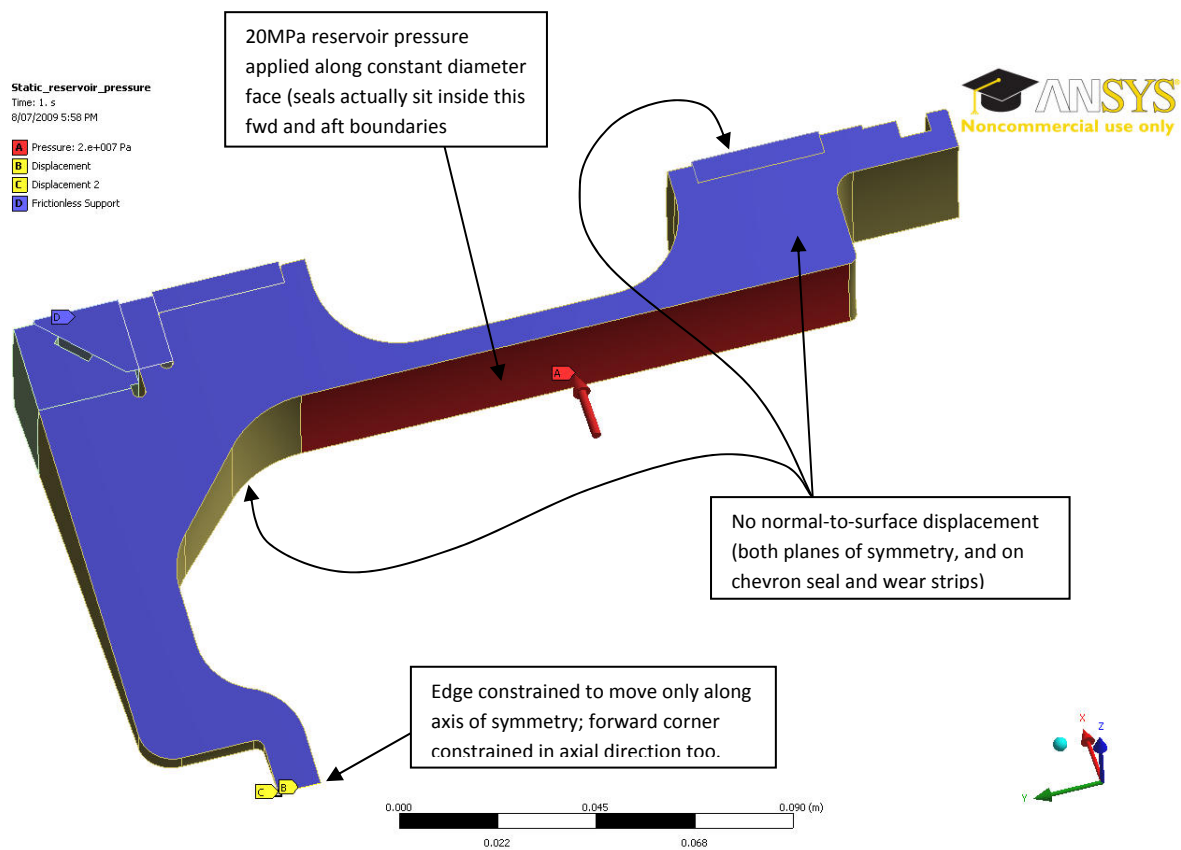


Figure 8: Loads and boundary conditions, 20 MPa reservoir pressure load case.

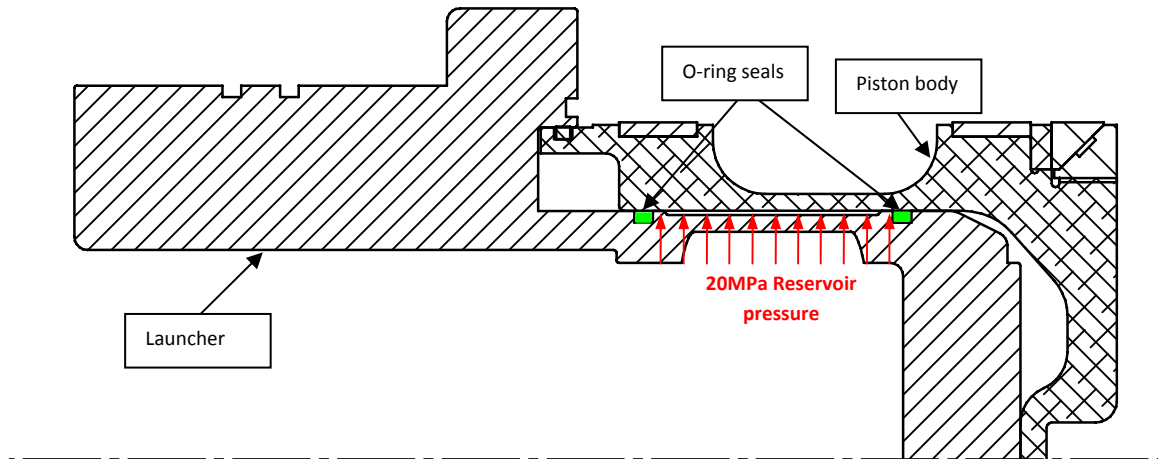


Figure 9: Piston launcher schematic.

### 6.3.5 Results

#### 6.3.5.1 80 MPa driver pressure loading

Figure 10 below shows a Von Mises stress plot for the piston assembly, using fully linear material properties. It can be seen that the peak stress (471 MPa) exceeds the yield stress allowable (414 MPa). All stresses exceeding yield are coloured red.

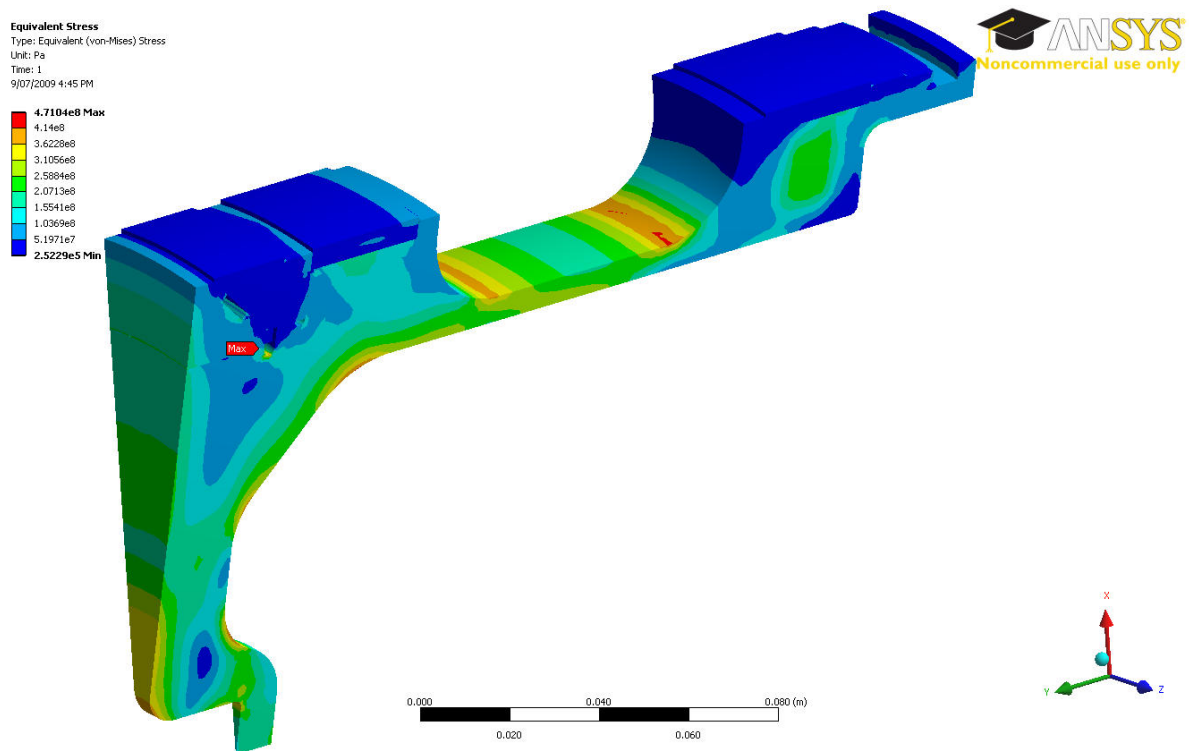
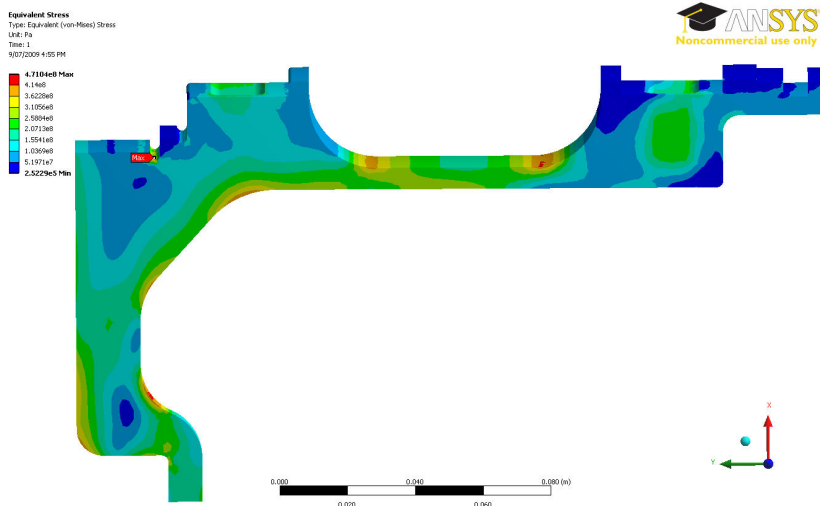


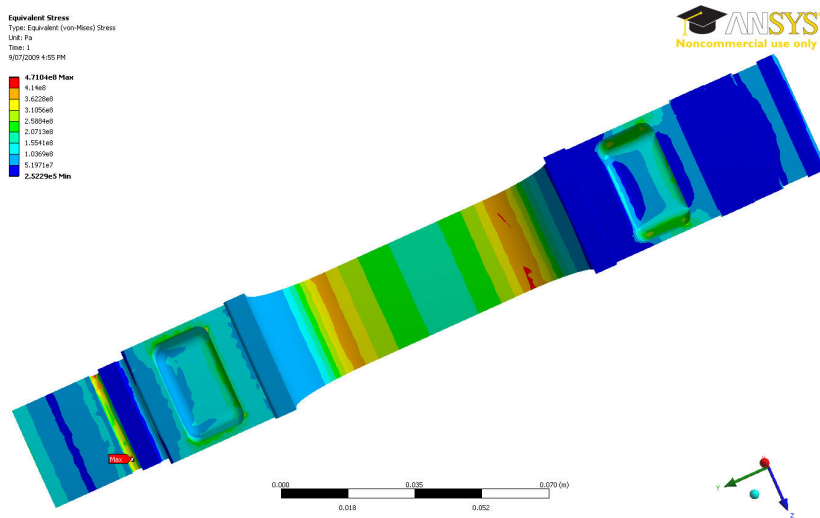
Figure 10: Von Mises stress distribution, 80 MPa driver pressure loading, linear materials.

It is clear in Figure 10 that only very localised patches on the surface are red, indicating that the actual component is unlikely to actually yield. However, to ensure failure does not occur, the model was re-run with non-linear material properties for the piston body (the accessory material properties remained linear).

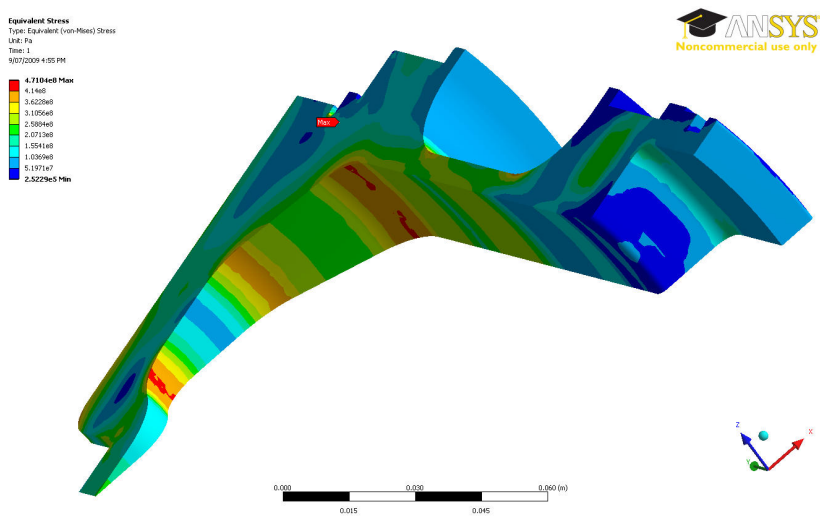
Figure 11 below shows multiple views of Von Mises plots calculated from the linear analysis, with red indicating stresses exceeding yield (414 MPa). Figure 12 shows multiple views of Von Mises plots calculated using a non-linear piston body material model, with red indicated stresses exceeding ultimate tensile levels (471 MPa). It is clear from Figure 12 that where yield stress was exceeded in Figure 11, that these loads redistribute in the non-linear model. Calculated stresses in the non-linear model do not exceed the ultimate tensile stress (471 MPa), therefore the piston will not fail.



(a) Side view

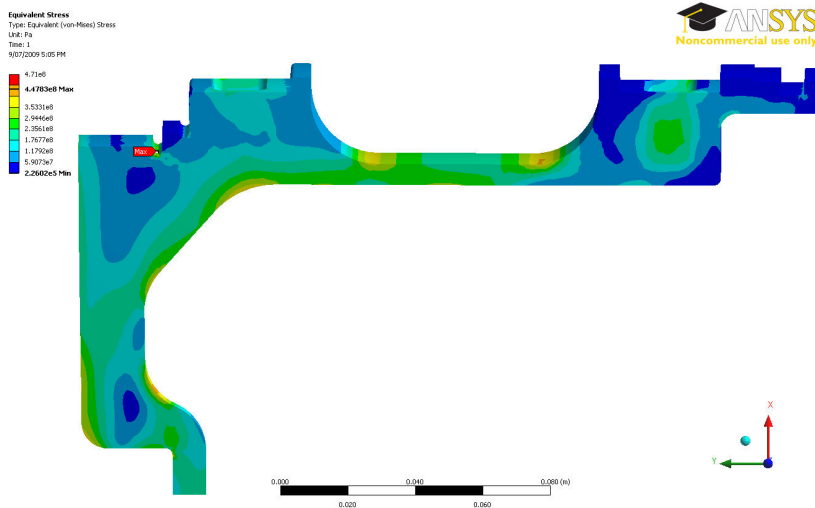


(b) Top view

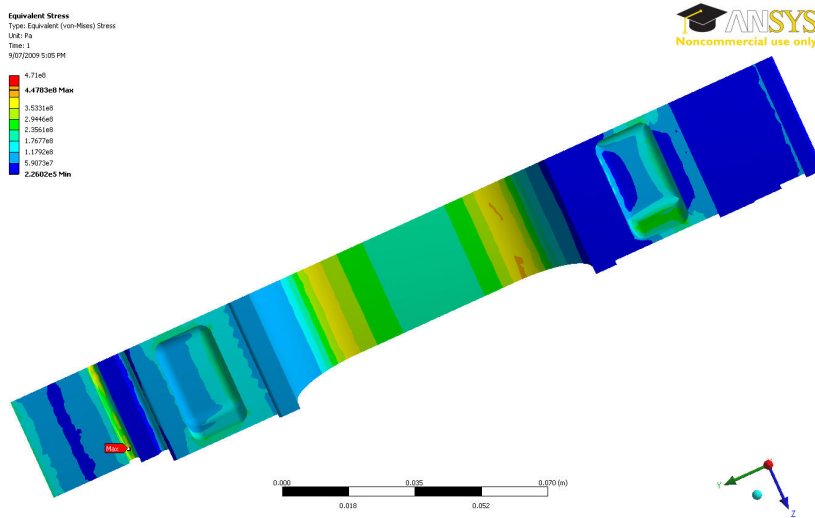


(b) Lower/rear view

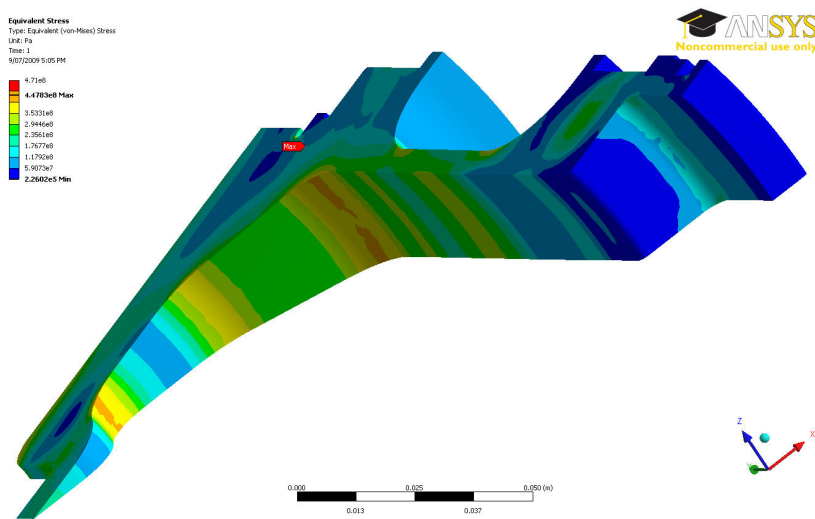
Figure 11: Von Mises stress distribution (Pa), linear piston body material model, 80 MPa driver pressure.



(a) Side view



(b) Top view



(b) Lower/rear view

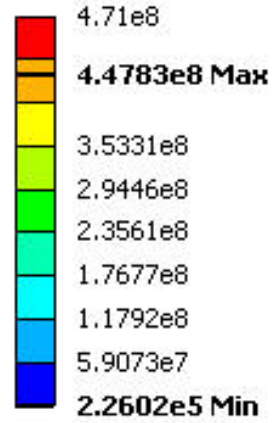
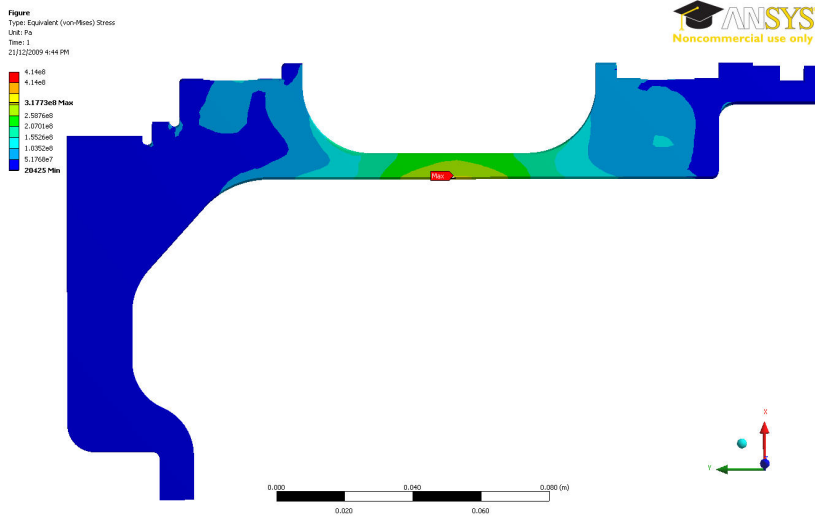


Figure 12: Von Mises stress distribution (Pa), nonlinear piston body material model, 80 MPa driver pressure.

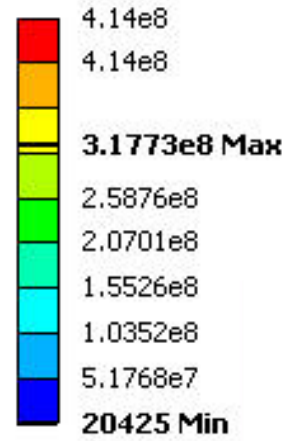
### ***6.3.5.2 20 MPa reservoir pressure loading***

Figure 13 below shows a Von Mises stress plot for the piston body. The model was run with fully linear materials. It can be seen that the yield stress is not exceeded and therefore the piston has sufficient strength to easily resist applied reservoir pressure loads.

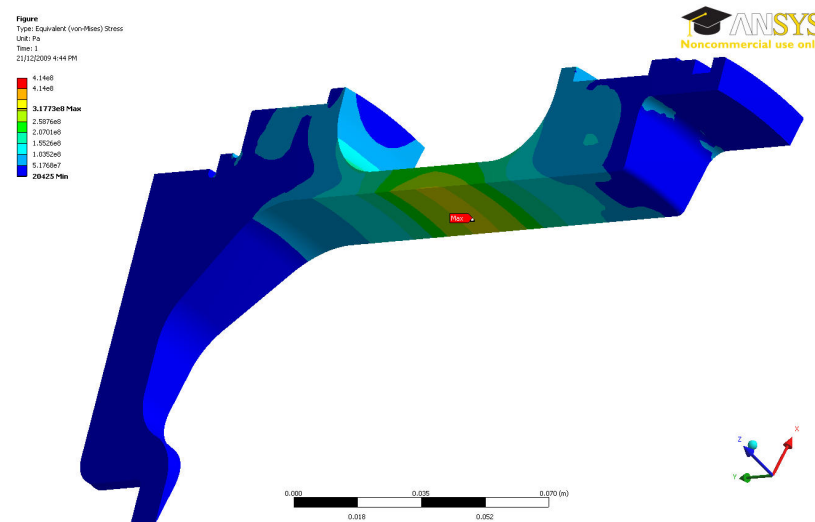
Figure 14 shows an exaggerated deformation plot for the piston body. It can be seen that the maximum displacement is approximately 0.3mm at the centre of the skirt, but approximately 0.1mm in the vicinity of the seals. Considering that actual reservoir pressures will be <10MPa, deflections around the seals will be <0.05mm, and therefore should not lead to leaking at the seals or interfacing problems.



(a) Side view



(b) Bottom view



(b) Lower/rear view

Figure 13: Von Mises stress distribution (Pa), linear piston body material model, 20 MPa reservoir pressure.



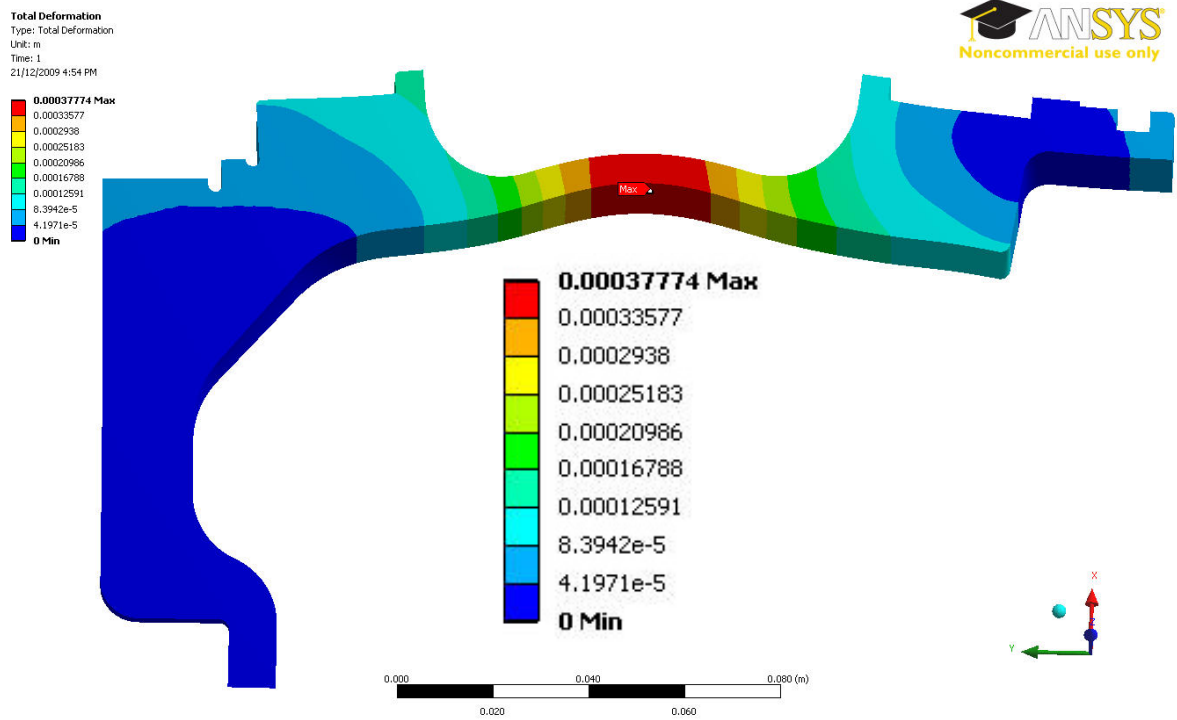


Figure 14: Piston deflection (m), linear piston body material model, 20 MPa reservoir pressure.

## 7 Analytical Stress Analysis

### 7.1 Overview

Some additional strength checks were performed using traditional stress analysis techniques. These checks are detailed in this section.

### 7.2 Buckling analysis

By inspection the thinned skirt on the piston is the most critical location for instability failure. Referring to the piston drawings in Appendix A, dimensions of the cylinder are as follows:

- Mean radius,  $r = \frac{203 + 190}{2 \times 2} = 98.25\text{mm}$ .
- Thickness,  $t = \frac{203 - 190}{2} = 6.5\text{mm}$ .
- Length,  $L = 152 - 66 = 86\text{mm}$  (this length conservatively includes both 20mm radii).

By inspection the column is short, and therefore will not fail by column buckling. However, it is still necessary to assess the piston for axi-symmetric instability failure (refer Figure 15). A simply but accurate methodology to calculate this stress is not available. However, a conservative approximation is now determined based on Roark [5], Table 15.2, Case 15, for local elastic instability failure of thin-walled circular tubes under uniform compression. Critical compressive stress due to local instability,  $\sigma_{cr}$ , is calculated as follows:

$$\sigma_{cr} = \frac{1}{\sqrt{3}} \frac{E}{\sqrt{1-\nu^2}} \frac{t}{r} \quad (1)$$

applicable for  $\frac{r}{t} > 10$  (thin walled) and  $L > 2 \times 1.72\sqrt{rt}$  (i.e.  $L >$  a single buckling wavelength)

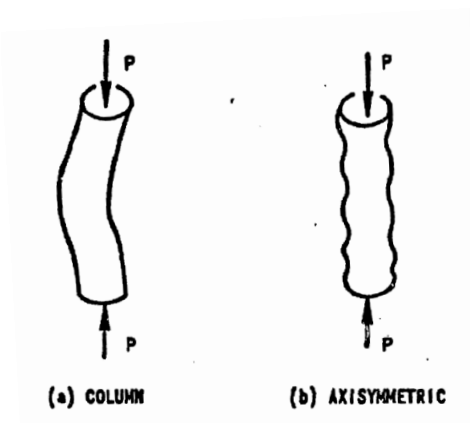


Figure 15: Von Column instability modes (taken from [6]).

Referring to Equation (1), and considering the geometry of the piston,  $\frac{r}{t} = \frac{98.25}{6.5} = 15.1 > 10$ , therefore the cylinder may be considered to be thin walled.

However,  $2 \times 1.72\sqrt{rt} = 2 \times 1.72\sqrt{98.25 \times 6.5} = 86.9 < L$ , which indicates that the piston skirt is slightly shorter than the actual wavelength associated with the instability failure. This indicates that the cylinder is probably too short to fail by local instability. However, the failing stress will still be calculated to ensure this mode of failure is not critical.

Substituting material properties from Table 1 and the above geometric properties into Equation (1):

$$\sigma_{cr} = \frac{1}{\sqrt{3}} \frac{71 \times 10^9}{\sqrt{1 - 0.33^2}} \frac{6.5}{98.25} = 2,873 \text{ MPa} \quad (2)$$

Roark [5] states that the stress calculated in Equation (2) should be scaled by 0.4-0.6 for an actual failing stress, giving  $\sigma_{cr} = 0.4 \times 2,873 \text{ MPa} = 1,149 \text{ MPa}$ . Clearly, since this stress far exceeds the material yield stress (414 MPa), and considering the conservative assumptions underlying this calculation, the piston will not fail due to local instability.

### 7.3 Reservoir Hoop Stress Finite Element Model Validation

Since hoop stress is easily estimated, it serves as a useful basis to validate the finite element model. Considering the minimum thickness section along the piston skirt, and the 20MPa reservoir pressure, hoop stress is now determined.

A schematic of a thin walled pressure vessel and the formula for hoop stress are shown in Figure 16 below. Substituting the mean piston wall thickness, and the 20MPa reservoir pressure, the idealised hoop stress may be determined:

$$\sigma_H = \frac{pD}{2t} = \frac{PD_i}{(D_i - D_o)} = \frac{20 \times 10^6}{(203 - 190)} 190 = 292 \text{ MPa} \quad (3)$$

Comparison of Equation (3) with Figure 13 indicates good correlation (292 MPa from classical analysis compared to 318 MPa from finite element analysis). This provides confidence in the geometric, material and load description in the finite element model.

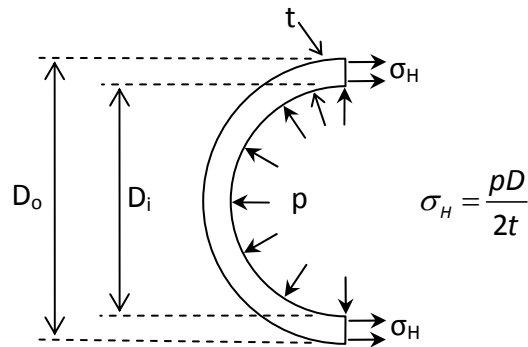


Figure 16: Hoop stress calculation – LC2.

## 7.4 Piston Impact

The piston has not been assessed for impact into the end of the tube. It was not considered feasible to design a lightweight piston which could sustain significant impact velocities into metal. Instead, an intrinsic limitation of the piston is that driver conditions must be designed such that impact into the end of the tube is avoided.

During initial development of new driver conditions for the lightweight piston, sacrificial nylon rods will be used to absorb piston kinetic energy if it still has significant velocity when it reaches the end of the tube. Anecdotal experience with free piston drivers at the Centre for Hypersonics indicates that this method is effective even with the much heavier pistons typically used in the facility, and should prove at least as effective for a much lighter piston.

Once the driver has been configured with the lightweight piston, a reusable rubber buffer will be utilised to catch the piston. The rubber buffer is incapable of absorbing significant amounts of kinetic energy, and therefore only low impact speeds are permissible (typically < 10m/s).

There remains the possibility that the lightweight piston may accidentally hit the end of the tube at high speed, most likely due to either operator error or unintentional pre-launch. If this occurs, the piston will almost certainly be irreparably damaged, and the primary concern is instead that the facility can contain the impact, and that operators are not injured. It is noted that the facility has been designed to safely contain impact of heavy solid pistons (including the 35kg X2 piston) into the end of the tube. By comparison, the lightweight piston presents a less severe impact case, for two reasons:

1. For a given impact velocity it has significantly less kinetic energy due to its lighter mass.
2. It is much more likely to be able to absorb impact energy through deformation of its thinner side walls.

## 7.5 Dynamic Pressure Loading

This analysis only considers static loading. In reality, driver pressure loading on the piston is characterised by very rapid ramping upwards of applied pressure loading to the front face of the piston, for a very short duration (<1 ms). Time constraints prevented detailed investigation of the dynamic stress response of the piston using explicit finite element solvers such as LS Dyna or AUTODYN. Instead, it is expected that the large safety factor (2x) should provide coverage for assumptions made by performing a static analysis. Additionally, detailed material properties at high strain rates could not be readily sourced for the piston alloy used.

Some preliminary dynamic analyses of ramped driver pressure loading using the ANSYS implicit solver indicated that peak stresses were momentarily approximately double those calculated by static analysis. However, these stresses had a duration in the order of microseconds, and therefore present a significantly different failure problem. Whilst this analysis has not accounted for this type of loading, two factors provide confidence that the current design is structurally safe:

1. The 2x safety factor applied to stresses, and the selection of conservative static material allowables, both provide a large margin of safety to accommodate the assumption of static loading.
2. Typically metals exhibit increased strength at very high strain rates. Referring to Johnson ([7], pages 132-133), below the recrystalline temperature of most metals and for large strains (0.05 to 0.5), the ratio of dynamic yield stress,  $\sigma_d$ , to static yield stress,  $\sigma_s$ , is approximately  $1 < \sigma_d / \sigma_s < 2$ ; that is to say, low temperature metals typically demonstrate higher strength at high strain rates. At high temperatures, this ratio increases significantly [7]. Whilst Aluminium is generally considered to have a relatively low strain sensitivity [8], it still demonstrates the same trend towards higher yield strength at high strain rates. Therefore the higher material strength at high strain rates will at least partially compensate for higher transient stresses that may occur.

## 7.6 Fatigue

The piston has not been assessed for fatigue failure. The nature of the applied loading is that it is high magnitude, but with a low number of cycles, so fatigue failure is not a primary concern. The piston will be examined regularly during testing to identify cracks or other evidence of damage. If evidence of fatigue cracking emerges, then more effort will be directed to determining the fatigue properties of the piston.

## 8 Operational Experience

A piston was manufactured in accordance with the Appendix A drawing set. Final manufactured mass was 10.524kg, which was approximately 1.5% lighter than the estimated mass. At the time of writing the piston had been used for 16 shots, with a measured peak driver pressure of 27.33MPa (shot x2s1300). After this initial test campaign, the piston was removed from the tunnel and inspected. There were no visible signs of damage. Driver pressures will be increased to approximately 40MPa during the next campaign, planned for January 2010, after which the piston will be re-examined for damage and general condition.



Figure 17: Newly manufactured piston, mass = 10.524kg.



**Figure 18: Piston undamaged after 9 shots.**

## **9 Recommendations**

The major deficiency identified in this analysis is the failure to accurately quantify and assess the piston structural response to dynamic loading, from both driver pressure loads, and also impact of the piston into the buffer/tube end. Future work would involve developing analysis techniques using an explicit finite element solver such as LS Dyna or AUTODYN to better understand the piston response to these applied loads. Such analyses would equally depend on obtaining accurate and representative material property data for high strain rate loading.



## 10 Conclusion

A new lightweight piston has been designed for X2. The piston will be used to develop a tuned free piston driver condition which should increase the useful supply time of driver gas. The new piston retains the interfacing geometry of the existing 35kg piston, but has had significant amounts of mass removed where practical.

The piston strength was assessed for two load cases: an 80MPa ultimate pressure load applied to the front face of the piston to represent driver gas loading, and a 20MPa reservoir pressure loading applied inside the piston to represent pressure loading for the piston on the launcher. The piston was analysed using a symmetric solid finite element model.

The 80 MPa driver pressure load case was shown to be critical. The Von Mises stress was determined to be generally less than the allowable yield stress of the piston. Some locations on the solid model had stresses slightly exceeding the yield stress. The model was therefore reanalyzed using a non-linear material model, where it was shown that peak stresses fell below the ultimate allowable stress in all places.

The piston was shown to be able to resist the 20MPa reservoir pressure loading with minimal deformation (<0.05mm) at the seals, thus avoiding pre-launch due to leakage.

The piston was not assessed for impact or dynamic pressure loading. The design relies on avoiding piston impact into the end of the tube at high velocities. If this occurs, the tube will contain the piston, but the piston is likely to be irreparably damaged. The 2x safety factor applied in static analyses is expected to provide coverage against higher stresses that may occur under the actual dynamic pressure loading conditions. Further, the piston material is expected to have higher strength at high strain rates, which will provide further protection against failure.

Initial testing to approximately 68% of limit load (27MPa peak driver pressure) demonstrated no structural damage to the piston. Further testing will increase applied loading to 100% of limit load (40MPa peak driver pressure), whereupon the piston will be re-examined.


It is recommended that future work should involve detailed analysis of the piston response to dynamic pressure and impact loading using an explicit finite element code. Coupled with accurate material properties for high strain rate loading, this will provide a better understanding of the response of the piston to the applied loads, permitting a more optimised design in future.

## 11 References

1. Dennis, C., *X2 Single Driver Solid Edge Drawing Set*. July 2002, Centre for Hypersonics, University of Queensland.
2. *U.S. Department of Defense - Military Handbook - MIL-HDBK-5G - Metallic Materials and Elements for Aerospace Vehicle Structures*. 1994.
3. *Copper and copper alloys*. 1st ed. ASM Speciality Handbook, ed. J.R. Davis. 2001, USA: ASM International.
4. Gere, J.M., Timoshenko, S.P., *Mechanics of Materials*. 4th SI ed. 1999, Cheltenham UK: Stanley Thornes.
5. Young, W.C. and R.G. Budynas, *Roark's Formulas for Stress and Strain*. 7th ed. 2002, Singapore: McGraw Hill.
6. Griffin, D.S., *Inelastic and Creep Buckling of Circular Cylinders due to Axial Compression, Bending, and Twisting*. December 1973, Westinghouse Electric Corporation, Advanced Reactors Division: Pittsburgh, P.A.
7. Johnson, W., *Impact Strength of Materials*. 1st ed. 1972, London: Edward Arnold.
8. R. Smerd, S.W., C. Salisbury, M. Worswick, D. Lloyd, M. Finn, *High strain rate tensile testing of automotive aluminum alloy sheet*. International Journal of Impact Engineering, 2005. 32: p. 20.

# Appendix A: Lightweight piston drawing set

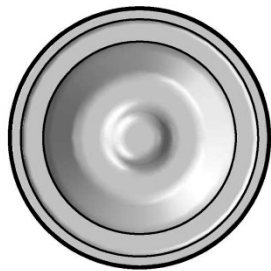
DRAFTING STANDARD: AS1100 - 1992  
DO NOT SCALE



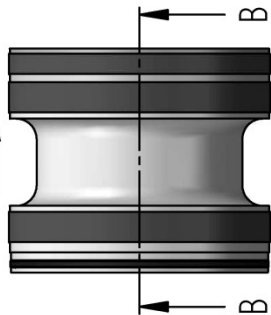
REVISION HISTORY

REV	DESCRIPTION	DATE	APPROVED
1	PN0. X2-LWP-001-0 changed to X2-LWP-001-1. Change involves modified cutout geometry. See drawing X2-LWP-001-1 for details.	21/10/2009	n/a

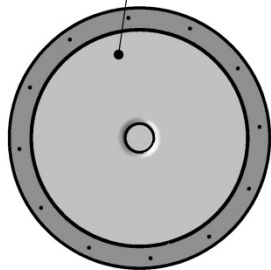
**PRINT ON A3 SHEETSIZE**



REAR VIEW



SIDE VIEW

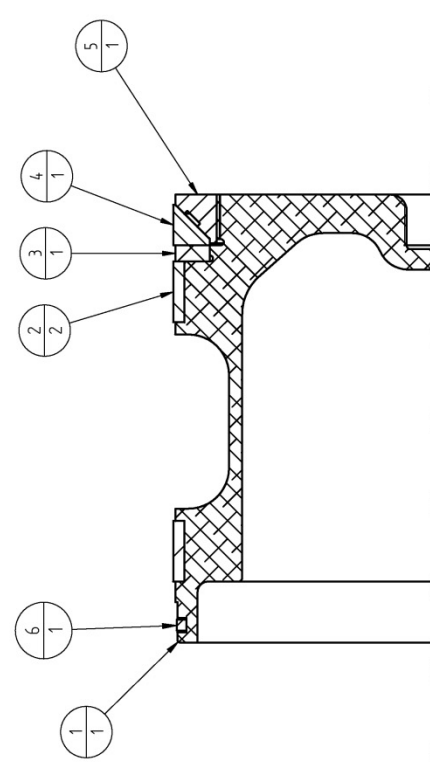


FRONT VIEW

Notes:

- Assemble Items 1 to 6 as shown.
- If necessary, Item 2 (fwd and aft wear rings) may be installed by first cutting a 45 deg diagonal split in the ring. The split ring can then be located at the correct position on the piston and bonded together using commercial araldite.
- Item 2 (wear rings) and Item 4 (chevron seal) are nominally oversized by 1mm diameter compared to the nominal X2 tunnel bore diameter of 256.8mm. Following assembly of the piston, the wear rings and chevron seal are to be machined to a diameter which results in 0.1mm total diametric clearance of the piston within the actual X2 tunnel. The piston should have a secure fit but still be able to slide freely within the tunnel.

Item Number	Document Number	Revision	Title	Material	Quantity	Mass
1	X2-LWP-001	1	X2 Lightweight piston body	Aluminium, 7075-T6 Rod	1	8.104 kg
2	X2-LWP-002	0	Wear ring	Oil Filled Nylon 6, Cast	2	0.297 kg
3	X2-LWP-003	0	Load ring	Commercial Aluminium	1	0.285 kg
4	X2-LWP-004	0	Chevron seal	Oil Filled Nylon 6, Cast	1	0.188 kg
5	X2-LWP-005	0	Brass holder	Aluminium Bronze L95810	1	1.789 kg
6	BS375	n/a	BS series o-ring	Nitrile	1	0.020 kg



SECTION B-B  
1:2

NAME	DATE
DRAWN: D. Gildford	10/21/09
CHECKED:	
ENG APPR:	
MGR APPR:	

CENTRE FOR HYPERSONICS  
THE UNIVERSITY OF QUEENSLAND

SIZE	DWG NO	REV
A3	X2-LWP-000	1

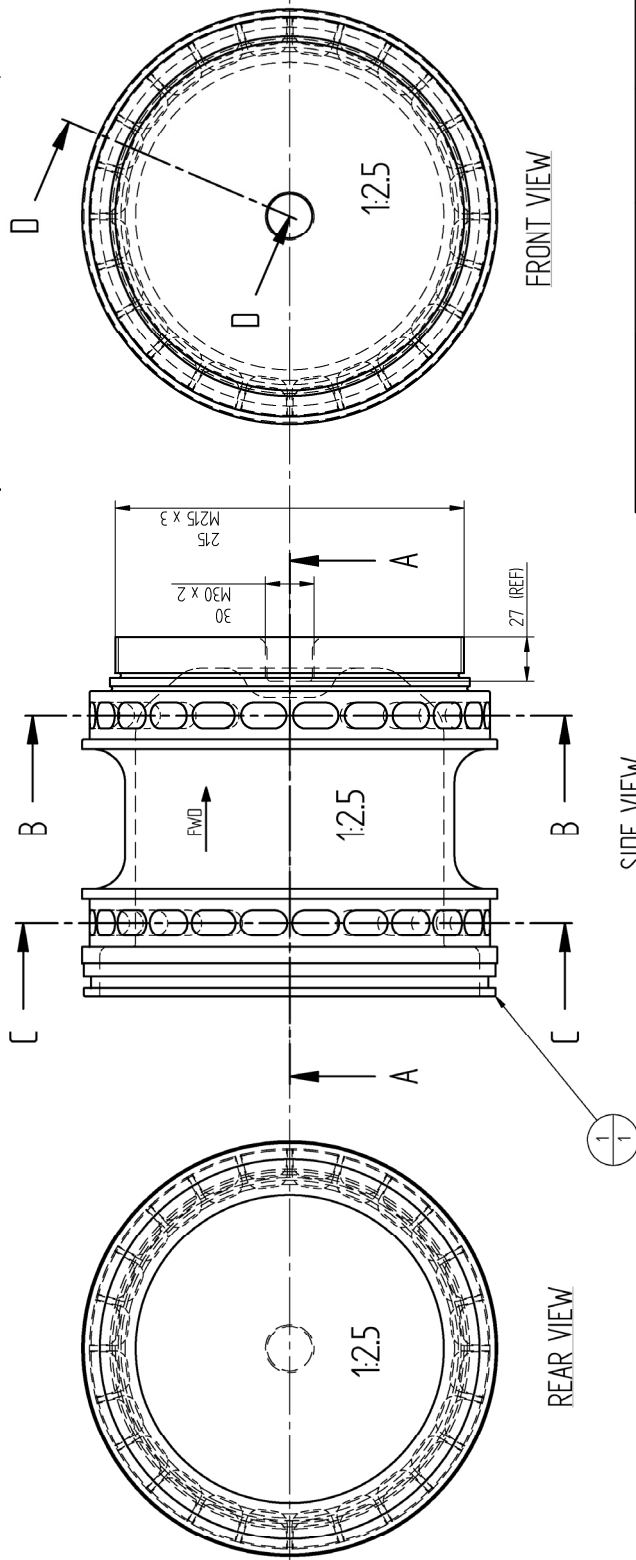
UNLESS OTHERWISE SPECIFIED  
DIMENSIONS ARE IN MILLIMETERS  
ANGULAR TOLERANCE ±0.1°  
DIMENSIONAL TOLERANCE ±0.1mm

SCALE: AS SHOWN WEIGHT: 10.683 kg SHEET 1 OF 1

DRAFTING STANDARD: AS100 - 1992  
DO NOT SCALE



REVISION HISTORY			
REV	DESCRIPTION	DATE	APPROVED
1	Geometry of cutouts beneath wear strips modified. Cutouts are now made using single 8mm radius.	21/10/2009	n/a



Item Number	Title	Material	Quantity
1	X2 lightweight piston body	Aluminum 7075-T6 Rod	1

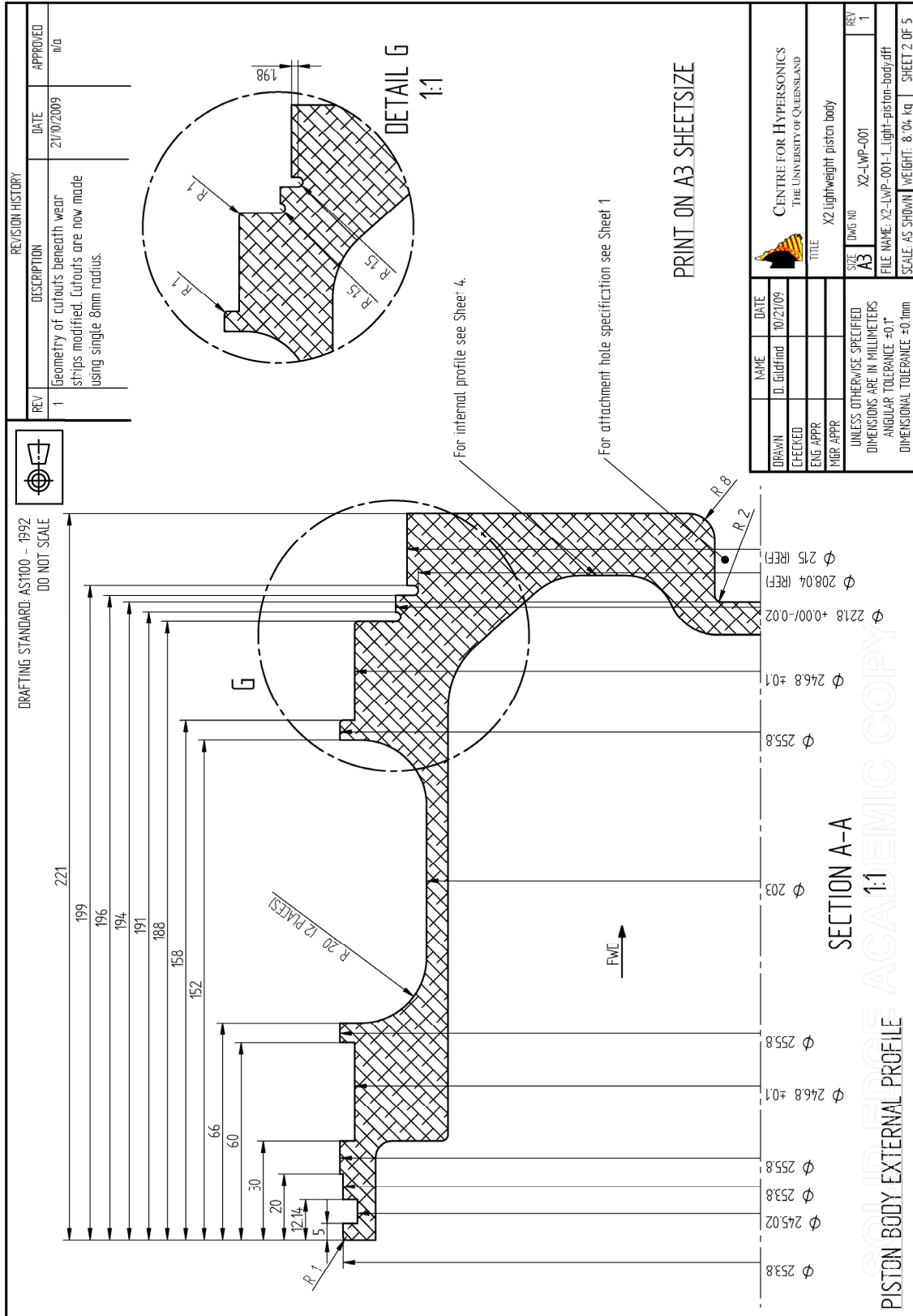
Notes:

1. Condition as supplied.
2. Surface finish as processed.
3. Surface treatment as processed.
4. Piston body outer profile is dimensioned on Sheet 2.
5. Piston body inner profile is dimensioned on Sheet 3.
6. Piston body outer surface cut-outs are dimensioned on Sheet 4.
7. Solid model views of the piston body are shown on Sheet 5.

PRINT ON A3 SHEET SIZE

ACADEMIC COPY

DRAWN	I. Gifford	DATE	10/21/09
CHECKED			
ENG APPR			
MGR APPR			
CENTRE FOR HYPERSONICS THE UNIVERSITY OF QUEENSLAND			
TITLE		X2 lightweight piston body	
UNLESS OTHERWISE SPECIFIED DIMENSIONS ARE IN MILLIMETERS ANGULAR TOLERANCE #0.1°	SIZE	DWG NO	REV
DIMENSIONAL TOLERANCE #0.1mm	A3	X2-LWP-001	1
FILE NAME: X2-LWP-001-Light-piston-body.dft			SHEET 1 OF 5
SCALE: AS SHOWN			WEIGHT: 8.04 kg

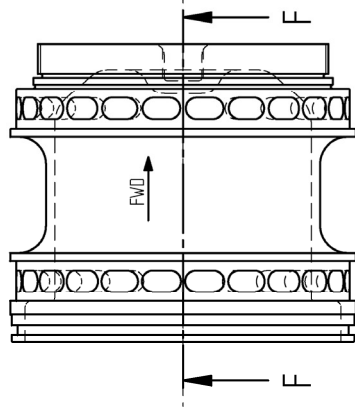
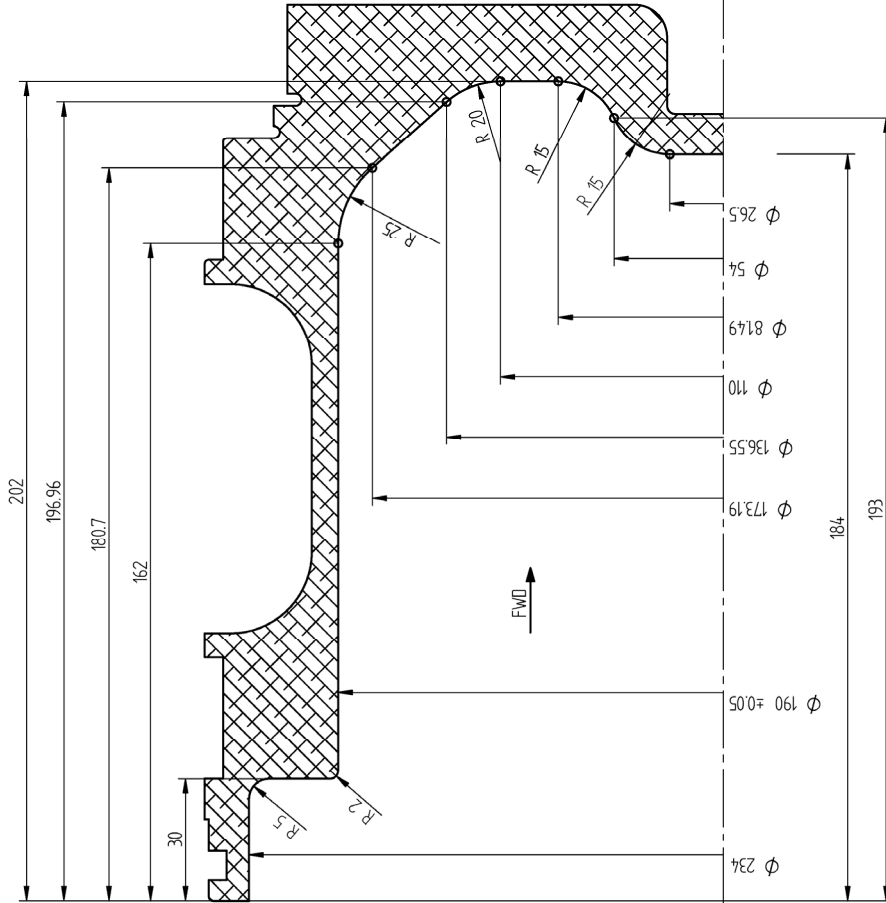


DRAFTING STANDARD: AS100 - 1992  
DO NOT SCALE



REVISION HISTORY

REV	DESCRIPTION	DATE	APPROVED
1	Geometry of cutouts beneath wear strips modified. Cutouts are now made using single 8mm radius.	27/07/2009	n/a



PRINT ON A3 SHEETSIZE

PISTON BODY INTERNAL PROFILE  
SECTION F-F

SOLID EDGE ACADEMIC 1:1 COPY

NAME	DATE
DRAWN: D. Gifford	10/21/09
CHECKED:	
ENG APPR:	
MGR APPR:	

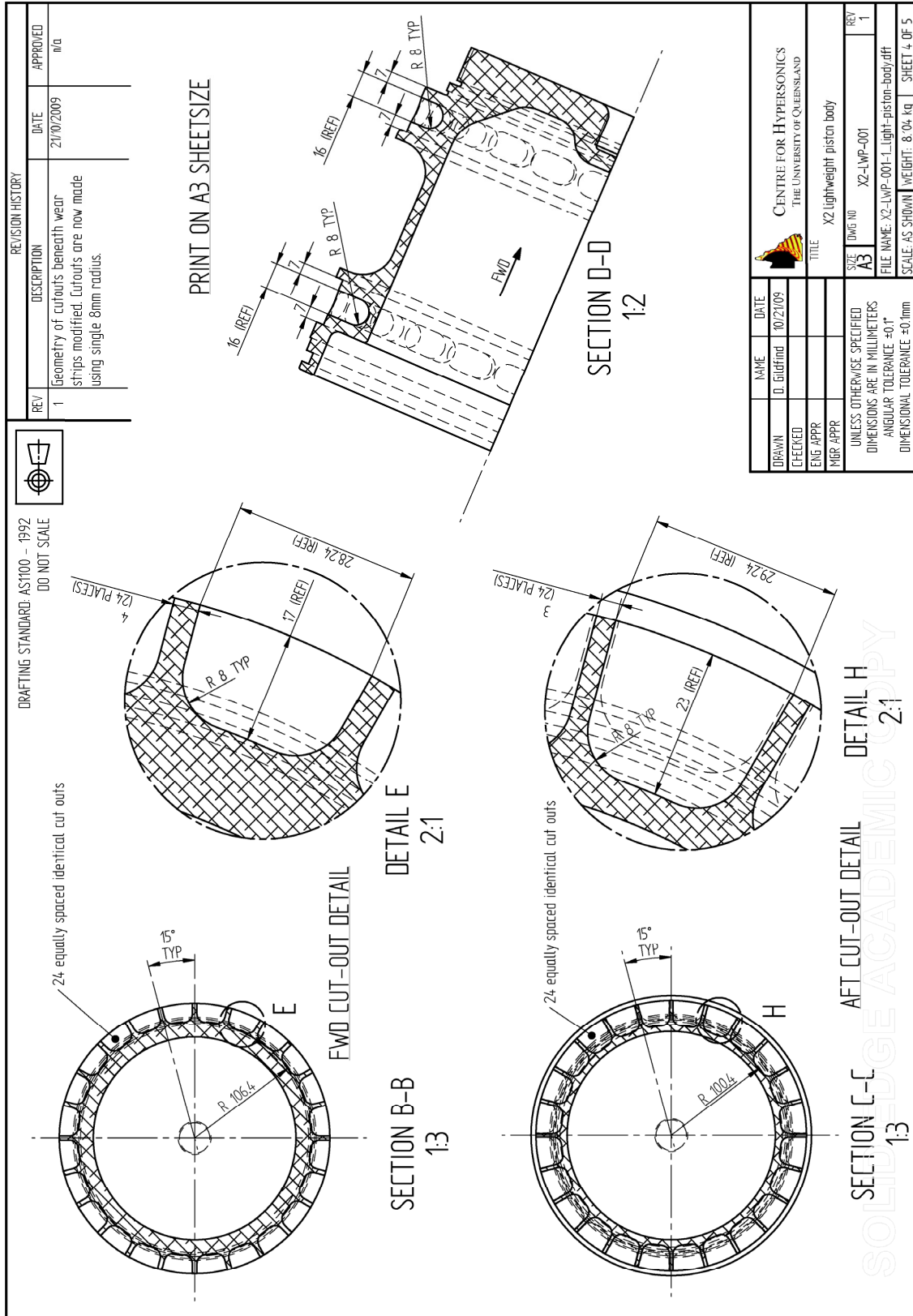
CENTRE FOR HYPERSONICS  
THE UNIVERSITY OF QUEENSLAND

TITLE: X2 Lightweight piston body

SIZE	DWG NO	REV
A3	X2-LWP-001	1

UNLESS OTHERWISE SPECIFIED  
DIMENSIONS ARE IN MILLIMETERS  
ANGULAR TOLERANCE  $\pm 0.1^\circ$   
DIMENSIONAL TOLERANCE  $\pm 0.1\text{mm}$

FILE NAME: X2-LWP-001-Light-piston-body.dft  
SCALE: AS SHOWN | WEIGHT: 8.04 kg | SHEET 3 OF 5

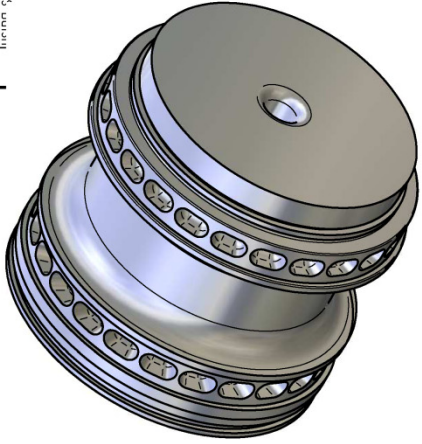




DRAFTING STANDARD: AS100 - 1992  
DO NOT SCALE



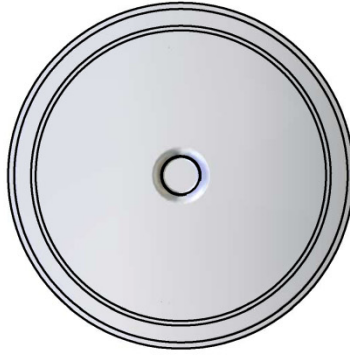
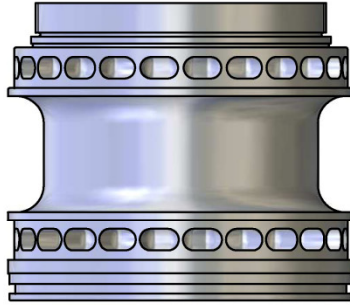
REVISION HISTORY			
REV	DESCRIPTION	DATE	APPROVED
1	Geometry of cutouts beneath wear strips modified. Cutouts are now made in one single 8mm radius.	21/10/2009	n/a



1:3



PRINT ON A3 SHEET SIZE



PISTON BODY SOLID MODEL VIEWS

DRAWN	I. Gifford	DATE	10/21/09
CHECKED			
ENG APPR			
MGR APPR			
UNLESS OTHERWISE SPECIFIED DIMENSIONS ARE IN MILLIMETERS ANGULAR TOLERANCE ±0.1° DIMENSIONAL TOLERANCE ±0.1mm		SIZE	A3
		DWG NO	X2-LWP-001
		REV	1
		FILE NAME	X2-LWP-001-Light-piston-body.dft
		SCALE AS SHOWN	WEIGHT: 8.104 kg SHEET 5 OF 5



CENTRE FOR HYPERIONICS  
THE UNIVERSITY OF QUEENSLAND

TITLE  
X2 Lightweight piston body

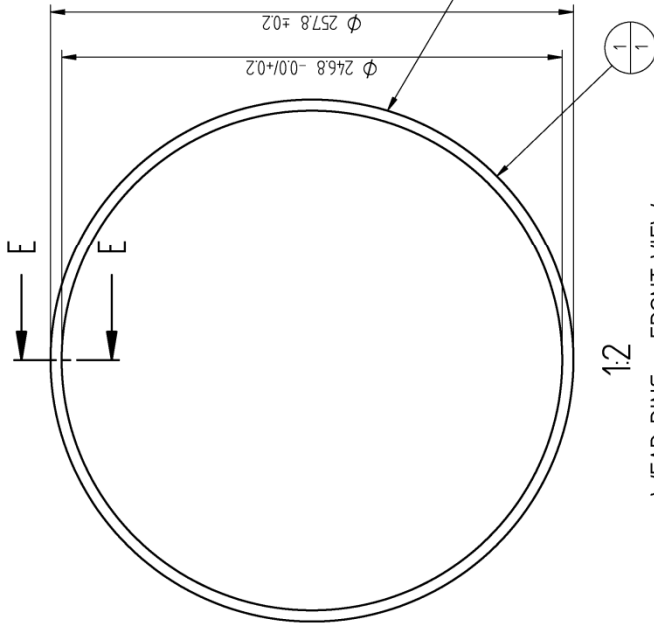
SOLID EDGE ACADEMIC COPY



DRAFTING STANDARD: AS1100 - 1992  
DO NOT SCALE



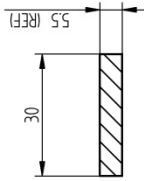
REVISION HISTORY			
REV	DESCRIPTION	DATE	APPROVED



1:2

WEAR RING - FRONT VIEW

Outer diameter is 1mm larger than X2 nominal tunnel bore diameter. Part is to be machined to X2 tunnel bore diameter nominally 256.8mm, permitting smooth sliding inside tunnel following chevron seal installation on the final piston assembly. Refer drawing X2-LWP-000 Rev 0.



SECTION E-E  
1:1

Item Number	Document Number	Title	Material	Quantity
1	X2-LWP-002	Wear ring	Oil Filled Nylon 6, Cast	1

NAME	DATE	<b>CENTRE FOR HYPERSONICS</b> THE UNIVERSITY OF QUEENSLAND	
DRAWN D. Gifford	07/02/09		
CHECKED		TITLE	
ENG APPR		SIZE	
MGR APPR		DWG NO	
UNLESS OTHERWISE SPECIFIED DIMENSIONS ARE IN MILLIMETERS ANGULAR TOLERANCE $\pm 0.1^\circ$ DIMENSIONAL TOLERANCE $\pm 0.1\text{mm}$		Wear ring	REV 0
		X2-LWP-002	FILE NAME: X2-LWP-002-0_wear-ring.dft
		SCALE: AS SHOWN	WEIGHT: 0.148kg
			SHEET 1 OF 1

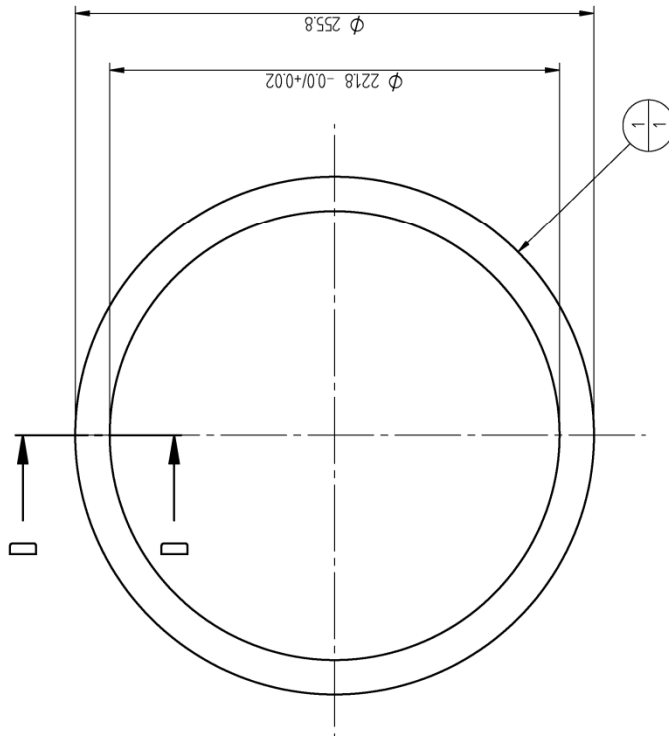
PRINT ON A3 SHEETSIZE

SOLID EDGE ACADEMIC COPY

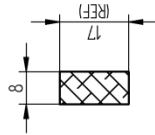
DRAFTING STANDARD: AS100 - 1992  
DO NOT SCALE



REVISION HISTORY			
REV	DESCRIPTION	DATE	APPROVED



1:2  
LOAD RING - FRONT VIEW



SECTION D-D  
1:1

Item Number	Document Number	Title	Material	Quantity
1	X2-LWP-003	Load ring	Commercial Aluminium	1

DRAWN	D. Giddford	DATE	07/02/09	 <b>CENTRE FOR HYPERSONICS</b> THE UNIVERSITY OF QUEENSLAND	
CHECKED					
ENG APPR					
MGR APPR					
UNLESS OTHERWISE SPECIFIED DIMENSIONS ARE IN MILLIMETERS ANGULAR TOLERANCE ±0.1° DIMENSIONAL TOLERANCE ±0.1mm				TITLE Load ring	
SIZE	A3	DWG NO	X2-LWP-003	REV	0
FILE NAME:	X2-LWP-003-0_Load-Ring.dft			SCALE:	AS SHOWN
WEIGHT:	0.285kg			SHEET 1 OF 1	

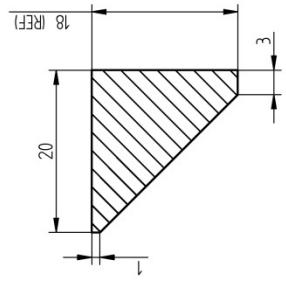
SOLID EDGE ACADEMIC COPY

PRINT ON A3 SHEETSIZE

REVISION HISTORY		DATE	APPROVED
REV	DESCRIPTION		

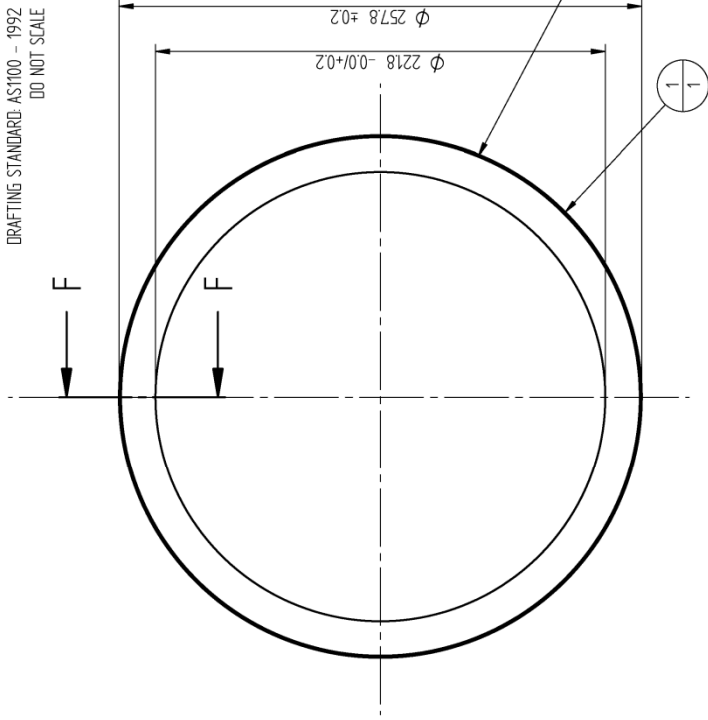


DRAFTING STANDARD: AS1100 - 1992  
DO NOT SCALE



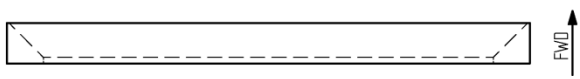
SECTION F-F  
2:1

Outer diameter is 1mm larger than X2 nominal tunnel bore diameter. Part is to be machined to X2 tunnel bore diameter (nominally 256.8mm, permitting smooth sliding inside tunnel) following chevron seal installation on the final piston assembly. Refer drawing X2-LWP-000 Rev 0.



1:2

FRONT VIEW



SIDE VIEW

Item Number	Document Number	Title	Material	Quantity
1	X2-LWP-004	Chevron seal	Oil Filled Nylon 6, Cast	1

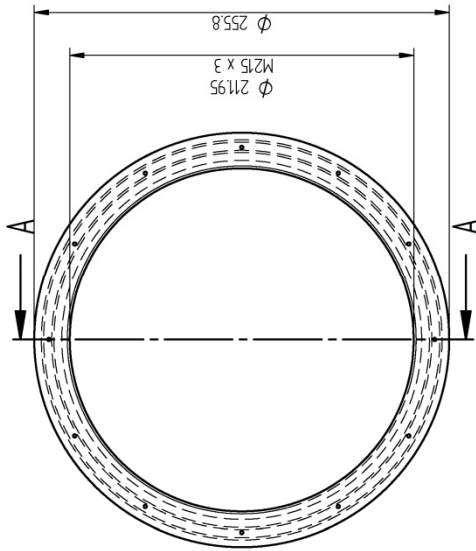
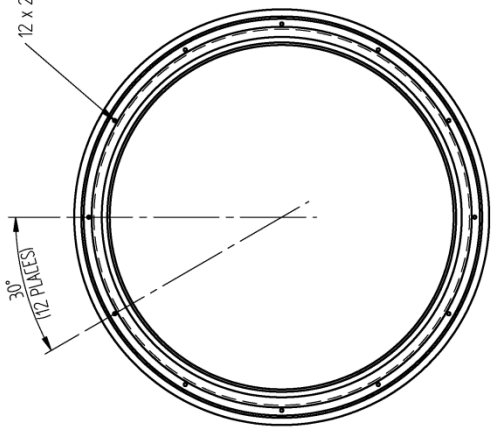
NAME	DATE	TITLE	SIZE	DWG NO	REV
DRAWN D. Giddford	07/02/09		A3	X2-LWP-004	0
CHECKED					
ENG APPR					
MGR APPR					
UNLESS OTHERWISE SPECIFIED DIMENSIONS ARE IN MILLIMETERS ANGULAR TOLERANCE $\pm 0.1^\circ$ DIMENSIONAL TOLERANCE $\pm 0.1mm$			FILE NAME: X2-LWP-004-0_chevron-seal.dwg		
CENTRE FOR HYPERSONICS THE UNIVERSITY OF QUEENSLAND			SCALE: AS SHOWN WEIGHT: 0.188kg SHEET 1 OF 1		

PRINT ON A3 SHEETSIZE  
SUNDRIDGE ACADEMIC COPY

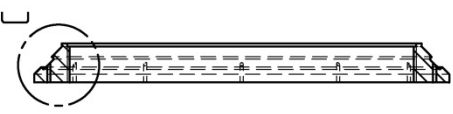
DRAFTING STANDARD: AS1000 - 1992  
DO NOT SCALE

REV	DESCRIPTION	DATE	APPROVED

12 x 2mm holes, spaced equally around circumference.



SECTION A-A



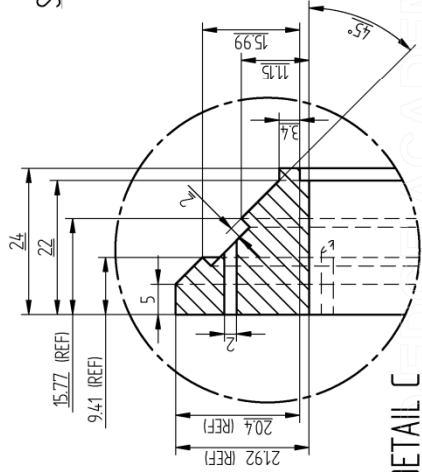
FRONT VIEW



FWD

1:2.5

SIDE VIEW



DETAIL C

15:1

Item Number	Document Number	Title	Material	Quantity
1	X2-LWP-005	Brass holder	Aluminium Bronze C95810	1

NAME	DATE	TITLE	SIZE	DWG NO	REV
DRAWN: D. Gildford	07/02/09	Brass holder	A3	X2-LWP-005	0
CHECKED:					
ENG APPR:					
MGR APPR:					

UNLESS OTHERWISE SPECIFIED  
DIMENSIONS ARE IN MILLIMETERS  
ANGULAR TOLERANCE ±0.1°  
DIMENSIONAL TOLERANCE ±0.1mm

SCALE: AS SHOWN WEIGHT: 1.789 kg SHEET 1 OF 1

PRINT ON A3 SHEET SIZE

SCIENTIFIC CAD

# Appendix B: 7075-T6 Rod Mechanical and Physical Properties

Refer: MIL-HDBK-5H, 1 December 1998, Table 3.7.4.0(d).

MIL-HDBK-5H  
1 December 1998

**Table 3.7.4.0(d). Design Mechanical and Physical Properties of 7075 Aluminum Alloy Bar, Rod, and Shapes: Rolled, Drawn, or Cold-Finished**

Specification	AMS 4122, AMS 4123, AMS 4186, AMS 4187, and AMS-QQ-A-225/9								AMS 4124 and AMS-QQ-A-225/9	
	Bar, rod, and shapes: rolled, drawn, or cold-finished									
Temper	T6, T651, and T62 <sup>a</sup>								T73 <sup>b,c</sup> or T7351 <sup>c</sup>	
Thickness <sup>d</sup> , in.	≤1.000		1.001-2.000		2.001-3.000		3.001-4.000		0.375-2.000	2.001-3.000
Basis	A	B	A	B	A	B	A	B	S	S
<b>Mechanical Properties:</b>										
$F_u$ , ksi:										
L	77	79	77	79	77	79	77	79	68	68
LT	77 <sup>e</sup>	79 <sup>e</sup>	75 <sup>e</sup>	77 <sup>e</sup>	72 <sup>e</sup>	74 <sup>e</sup>	69 <sup>e</sup>	71 <sup>e</sup>	...	65 <sup>e,f</sup>
$F_y$ , ksi:										
L	66	68	66	68	66	68	66	68	56	56
LT	66 <sup>e</sup>	68 <sup>e</sup>	66 <sup>e</sup>	68 <sup>e</sup>	63 <sup>e</sup>	65 <sup>e</sup>	60 <sup>e</sup>	62 <sup>e</sup>	...	52 <sup>e,f</sup>
$F_{0.2}$ , ksi:										
L	64	66	64	66	64	66	64	66	54	54
LT	...	...	...	...	...	...	...	...	...	55 <sup>f</sup>
$F_{0.01}$ , ksi:										
L	46	47	46	47	46	47	46	47	42	40
$F_{brs}$ , ksi:										
(e/D = 1.5)	100	103	100	103	100	103	100	103	101	101
(e/D = 2.0)	123	126	123	126	123	126	123	126	131	131
$F_{brs}$ , ksi:										
(e/D = 1.5)	86	88	86	88	86	88	86	88	81	81
(e/D = 2.0)	92	95	92	95	92	95	92	95	100	100
$e$ , percent (S-basis):										
L	7	...	7	...	7	...	7	...	10	10
$E$ , 10 <sup>3</sup> ksi	10.3									
$E_c$ , 10 <sup>3</sup> ksi	10.5									
$G$ , 10 <sup>3</sup> ksi	3.9									
$\mu$	0.33									
<b>Physical Properties:</b>										
$\omega$ , lb/in. <sup>3</sup>	0.101									
$C$ , $K$ , and $\alpha$	See Figure 3.7.4.0									

- a Design allowables were based upon data obtained from testing of T6 and T651 material and from samples of material, supplied in the O or F temper, which were heat treated to T62 temper to demonstrate response to heat treatment by suppliers.
- b Design allowables were based upon data obtained from testing T73 and T7351 temper material and from testing samples of material, supplied in the O or F temper, which were heat treated to T73 temper to demonstrate response to heat treatment by suppliers.
- c Bearing values are "dry pin" values per Section 1.4.7.1.
- d For rounds (rod) maximum diameter is 4 inches; for square bar, maximum size is 3½ inches; for rectangular bar, maximum thickness is 3 inches with corresponding width of 6 inches; for rectangular bar less than 3 inches in thickness, maximum width is 10 inches.
- e Caution: This specific alloy, temper, and product form exhibits poor stress-corrosion cracking resistance in this grain direction. It corresponds to an SCC resistance rating of D, as indicated in Table 3.1.2.3.1(a).
- f ST grain direction.

# Appendix C: DOTMAR Nylon 6 Oil Filled Cast Properties



**ENQUIRE NOW**

[www.dotmar.co.nz](http://www.dotmar.co.nz)

## Nylon 6 Oil Lubricated

### Product Description

Nylon 6 Oil Lubricated nylon is an internally lubricated nylon, which is self-lubricating in the real meaning of the word. Nylon 6 Oil Lubricated nylon, specifically developed for unlubricated moving parts components, gives a considerable enlargement of the use of nylons. This is because of its reduced friction (-50%) and increased wear resistance (up to 10X).

#### Features and Benefits:

- High strength
- Highly fatigue resistant
- Excellent mechanical damping
- Good sliding characteristics
- Good wear resistance

### Applications

Nylon plastic is used for a wide range of engineering components both for OEM's and maintenance. Some examples are:

- nylon sleeve bearings
- nylon slide bearings
- nylon wear blocks
- nylon support wheels
- nylon guide wheels
- nylon conveyor rollers
- nylon tensioner rollers
- nylon wheel sleeves
- nylon rollers sleeves
- nylon cams
- nylon buffer block
- nylon hammer heads
- nylon scrapers
- nylon gear wheels
- nylon sprockets
- nylon seal-rings

### Delivery Program

(Olive Green)



#### Nylon Sheet

Thickness: 8 - 100 mm  
Sizes: 1220 x 610, 2440 x 1220 mm



#### Nylon Rod

Outside Diameter: 50 - 300 mm



#### Nylon Tube

Outside Diameter: 50 - 500 mm



#### Machined Nylon Parts

### Physical Properties

<b>Specific Gravity</b> Units g/cm <sup>3</sup>	1.135
<b>Continuous Operating Temperature</b> Unit °C - 5,000Hrs / 20,000Hrs	105/90
<b>Tensile Strength</b> Units MPa	70
<b>Impact Resistance</b> Units Charpy KJ/m <sup>2</sup>	>50
<b>Impact Resistance</b> Units Izod KJ/m <sup>2</sup>	4
<b>Hardness</b> Units Rockwell M	82
<b>Co-efficient of Thermal Expansion</b> Units mm/(mmxK) x 10 <sup>-6</sup> avg value 23-60°C	80
<b>Dielectric Strength</b> Units KV/mm	22
<b>Surface Resistivity</b> Units Ohms	1x10 <sup>13</sup>
<b>Flammability</b> Oxygen Index %	-
<b>Flammability</b> UL94	HB
<b>FDA Approved</b> <a href="#">For a full list of ratings click here</a>	No



**Dotmar Engineering Plastics ... your partner in performance engineering plastics.**

[Print Data Sheet](#)

[View Property Comparison Table](#)

[E-mail this Page](#)

[Close Window](#)

# Appendix D: MATWEB Nylon 6 Oil Filled Cast Properties

Quadrant EPP Nylatron® LIG Nylon, Type 6, oil filled, cast

Page 1 of 2

## Quadrant EPP Nylatron® LIG Nylon, Type 6, oil filled, cast

**Categories:** [Polymer](#); [Thermoplastic](#); [Nylon](#); [Nylon 6](#); [Nylon 6, Glass Fiber/Solid Lube Filled](#)

**Material Notes:** Information provide by Quadrant Engineering Plastics Products.

**Key Words:** Polyamide

**Vendors:** [Click here to view all available suppliers for this material.](#)

Please [click here](#) if you are a supplier and would like information on how to add your listing to this material.

Physical Properties	Metric	English	Comments
Specific Gravity	1.14 g/cc	0.0412 lb/in <sup>3</sup>	ASTM D792
Water Absorption	0.300 %	0.300 %	Immersion, 24hr; ASTM D570(2)
Water Absorption at Saturation	6.00 %	6.00 %	Immersion; ASTM D570(2)
Mechanical Properties	Metric	English	Comments
Hardness, Rockwell M	85	85	ASTM D785
Hardness, Rockwell R	120	120	ASTM D785
Tensile Strength, Ultimate	68.3 MPa	9900 psi	ASTM D638
Elongation at Break	50.0 %	50.0 %	ASTM D638
Tensile Modulus	3.21 GPa	465 ksi	ASTM D638
Flexural Modulus	3.62 GPa	525 ksi	ASTM D790
Flexural Yield Strength	103 MPa	15000 psi	ASTM D790
Compressive Strength	93.1 MPa	13500 psi	10% Def.; ASTM D695
Compressive Modulus	2.28 GPa	330 ksi	ASTM D695
Shear Strength	64.1 MPa	9300 psi	ASTM D732
Coefficient of Friction	0.140	0.140	Dry vs. Steel; QTM55007
K (wear) Factor	181 x 10 <sup>-8</sup> mm <sup>3</sup> /N-M	90.0 x 10 <sup>-10</sup> in <sup>3</sup> -min/ft-lb-hr	QTM 55010
Limiting Pressure Velocity	0.210 MPa-m/sec	6000 psi-ft/min	4:1 safety factor; QTM 55007
Izod Impact, Notched	0.534 J/cm	1.00 ft-lb/in	ASTM D256 Type A
Thermal Properties	Metric	English	Comments

CTE, linear	101 $\mu\text{m/m}\cdot^\circ\text{C}$ @Temperature -40.0 - 149 $^\circ\text{C}$	56.0 $\mu\text{in/in}\cdot^\circ\text{F}$ @Temperature -40.0 - 300 $^\circ\text{F}$	ASTM E831
Melting Point	216 $^\circ\text{C}$	420 $^\circ\text{F}$	Crystalline, Peak; ASTM D3418 Long Term
Maximum Service Temperature, Air	104 $^\circ\text{C}$	220 $^\circ\text{F}$	
Deflection Temperature at 1.8 MPa (264 psi)	93.3 $^\circ\text{C}$	200 $^\circ\text{F}$	ASTM D648
Flammability, UL94	HB	HB	1/8 inch (Estimated Rating)

**Descriptive Properties**

Compliance - FDA	Not Compliant	
Machinability	2	1-10, 1=Easier to Machine
Service in Alcohols	Limited	
Service in Aliphatic Hydrocarbons	Acceptable	
Service in Aromatic Hydrocarbons	Acceptable	
Service in Chlorinated Solvents	Limited	
Service in Ethers	Acceptable	
Service in Ketones	Acceptable	
Service in Strong Acids	Unacceptable	
Service in Strong Alkalis	Unacceptable	
Service in Sunlight	Limited	
Service in Weak Acids	Limited	
Service in Weak Alkalis	Limited	

Some of the values displayed above may have been converted from their original units and/or rounded in order to display the information in a consistent format. Users requiring more precise data for scientific or engineering calculations can click on the property value to see the original value as well as raw conversions to equivalent units. We advise that you only use the original value or one of its raw conversions in your calculations to minimize rounding error. We also ask that you refer to MatWeb's disclaimer and terms of use regarding this information. [Click here](#) to view all the property values for this datasheet as they were originally entered into MatWeb.



# Appendix E: X2 Lightweight Piston Initial Blanked Off Shot Details (Extract From Unpublished Test Report)

Shot ID [-]	Date [-]	Case ID [-]	Scale Factor <sup>1</sup> [-]	$p_{res,0}$ [MPa]	$p_{D,0,He}$ [kPa]	$p_{D,0,Ar}$ [kPa]	Rebound <sup>2</sup> [mm]	$\lambda$ [-]	$p_{max}^{10}$ [MPa]	$u_{p,max}$ [m/s]	$n$ [-]	Results reference [-]
x2s1293	20/11/09	1	0.75	0.80	0.0	14.0	50 <sup>3</sup>	71.5	18.43	145	1.68	Figure 92 on page 128
x2s1294	20/11/09	13	0.64	2.00	47.8	11.9	- <sup>4</sup>	-	-	-	-	-
x2s1295	20/11/09	13	0.64	2.00	47.8	11.9	- <sup>4</sup>	-	-	-	-	-
x2s1296	21/11/09	13	0.64	2.00	47.8	11.9	136 <sup>5</sup>	30.0	15.86	177	1.64	Figure 93 on page 129
x2s1297	21/11/09	13	1.00	3.12	74.6	18.6	169 <sup>5</sup>	24.5	19.82	219	1.68	Figure 94 on page 130
x2s1298	21/11/09	13	1.00	3.12	74.6	18.6	120 <sup>6</sup>	33.6	19.90	295	1.53 <sup>6</sup>	Figure 94 on page 130
x2s1299	21/11/09	29	0.50	3.03	66.3	7.4	109 <sup>6</sup>	36.7	24.72	224	1.61 <sup>6</sup>	Figure 95 on page 131
x2s1300	21/11/09	29	0.60	3.63	79.5	8.8	118 <sup>6</sup>	34.1	27.33	242	1.62 <sup>6</sup>	Figure 96 on page 132
x2s1301	23/11/09	29	0.60	3.63	79.5	8.8	139 <sup>7</sup>	29.4	27.31	241	1.70	Figure 96 on page 132
x2s1302	23/11/09	13	1.00	3.12	74.6	18.6	- <sup>8</sup>	-	-	-	-	-
x2s1303	23/11/09	13	1.00	3.12	74.6	18.6	175 <sup>7</sup>	23.7	19.76	235	1.69	Figure 94 on page 130
x2s1304	23/11/09	1	1.00	1.06	0.0	18.7	58 <sup>7</sup>	63.4	23.01	203	1.71	Figure 97 on page 133
x2s1305	23/11/09	1	1.00	1.06	0.0	18.7	60 <sup>7</sup>	61.6	21.87	189	1.71	Figure 97 on page 133
x2s1306	23/11/09	X2 Nominal	1.00	1.10	30.0	0.0	103 <sup>4</sup>	38.6	13.07	139	1.66	Figure 98 on page 134
x2s1307	24/11/09	X2 Nominal	1.80	1.98	54.0	0.0	125 <sup>4</sup>	32.4	17.88	214	1.67	Figure 99 on page 135 <sup>9</sup>
x2s1308	24/11/09	X2 Nominal	2.30	2.53	69.0	0.0	135 <sup>4</sup>	30.2	19.81	202	1.66	Figure 100 on page 136

<sup>1</sup> Scale factor is applied to driver and reservoir fill pressures.  
<sup>2</sup> This is the measured point of piston rebound, where velocity is zero, compression ratio is a maximum, and after which the piston then starts to accelerate back towards the reservoir.  
<sup>3</sup> Piston was observed to hit buffer (rods crushed against it), but did not hit hard (since no damage was evident).  
<sup>4</sup> Shot failed to trigger.  
<sup>5</sup> Piston rebound position measured from final position of deformable rods.  
<sup>6</sup> It appears that the piston hit the rods with sufficient velocity to give them inertia to continue moving towards the buffer, after the piston had already decelerated to a temporary stop before rebounding backwards. This would result in the volumetric compression ratio being over-estimated, and thus  $gamma_{eff}$  being underestimated (and therefore an inaccurate estimate of  $gamma_{eff}$  for the affected shots). Rod overshoot was only evident where rods extended significantly past the piston rebound point (and were therefore hit by the piston while it was at a high velocity).  
<sup>7</sup> Staggered rods, spaced at 1cm increments, were used. Piston rebound position was then determined from both impacted and unimpacted rods, as opposed to just the impacted rods. This permits cases of rod overshoot to be identified by the fact that impacted rods are in final deformed positions lying past the unimpacted rods. Thus, significant errors are avoided where piston rebound position would otherwise be overestimated.  
<sup>8</sup> Piston did not hit staggered rods due to insufficient rod length from buffer.  
<sup>9</sup> Tunnel was not fired in normal firing position. As a result, recoil sensor was orientation was not within normal range, and therefore output is reversed, uncalibrated, and therefore compromised.  
<sup>10</sup> Both a normal PCB (111A23-8483 in Table 13 on the previous page) and a ceramic coated PCB (either 118A-3054 or 118A-4266 in Table 13) were installed in the blank-off plate and used to measure driver pressure. Both ceramic PCBs recorded erroneous pressure traces. This is thought to be a result of the external amplification required for these transducers, coupled with excessively long cables. Therefore the normal PCB (111A23-8483) results have been used for data analysis.